Time-series measurements of ^{234}Th in water column and sediment trap samples from the northwestern Mediterranean Sea

J. Kirk Cochran[1*], Juan Carlos Miquel[2], Robert Armstrong[1], Scott W. Fowler[2], Pere Masqué[3], Beat Gasser[2], David Hirschberg[1], Jennifer Szlosek[1], Alessia M. Rodriguez y Baena[2], Elisabet Verdeny[3] and Gillian M. Stewart[1,4]

[1]Marine Sciences Research Center, Stony Brook University, Stony Brook, New York 11794-5000 USA

[2]Marine Environment Laboratories, International Atomic Energy Agency, 4 quai Antoine 1[er], Monaco

[3]Institut de Ciencia i Tecnologia Ambientals- Departament de Fisica, Universitat Autonoma de Barcelona, 08193 Bellaterra, Spain

[4]Department of Earth and Environmental Sciences, Queens College CUNY, Flushing, New York 11367 USA

***Corresponding author. Tel.: +1 631 632 8733; fax: +1 631 632 3066.**
***E-mail address*: kcochran@notes.cc.sunysb.edu**

Abstract

Disequilibrium between ^{234}Th and ^{238}U in water column profiles has been used to estimate the settling flux of Th (and, by proxy, of particulate organic carbon); yet potentially major non-steady-state influences on ^{234}Th profiles are often not able to be considered in estimations of flux. We have compared temporal series of ^{234}Th distributions in the upper water column at both coastal and deep-water sites in the northwestern Mediterranean Sea to coeval sediment trap records at the same sites. We have used sediment trap records of ^{234}Th fluxes to predict temporal changes in water column ^{234}Th deficits and have compared the predicted deficits to those measured to determine whether the time-evolution of the two coincide. At the coastal site (327 m water depth), trends in the two estimates of water column ^{234}Th deficits are in fairly close agreement over the one-month deployment during the spring bloom in 1999. In contrast, the pattern of water column ^{234}Th deficits is poorly predicted by sediment trap records at the deep-water site (DYFAMED, ~2300 m water depth) in both 2003 and 2005. In particular, the transition from a mesotrophic to an oligotrophic system, clearly seen in trap fluxes, is not evident in water column ^{234}Th profiles, which show high-frequency variability. Allowing trapping efficiencies to vary from 100% does not reconcile the differences between trap and water column deficit observations; we conclude that substantial lateral and vertical advective influences must be invoked to account for the differences.

Advective influences are potentially greater on ^{234}Th fluxes derived from water column deficits relative to those obtained from traps because the calculation of deficits in open-ocean settings is dominated by the magnitude of the "dissolved" ^{234}Th fraction. For observed current velocities of 5 – 20 cm s^{-1}, in one radioactive mean-life of ^{234}Th, the water column at the

DYFAMED site can reflect ^{234}Th scavenging produced tens to hundreds of kilometers away. In contrast, most of the ^{234}Th flux collected in shallow sediment traps at the DFYFAMED site was in the fraction settling >200 m d^{-1}; in effect the sediment trap can integrate the ^{234}Th flux over distances ~40-fold less than water column ^{234}Th distributions. In some sense, sediment trap and water column sampling for ^{234}Th provide complementary pictures of ^{234}Th export. However, because the two methods can be dominated by different processes and are subject to different biases, their comparison must be treated with caution.

Keywords: Thorium-234, particle fluxes, sediment traps, northwest Mediterranean, non-steady state

1. Introduction

Over the past ~20 years, the deficiency of the natural radionuclide ^{234}Th (half-life 24.1 d) with respect to its parent ^{238}U in the upper water column has increasingly been used to determine the export of particulate organic carbon (POC) from the photic zone (see Cochran and Masqué, 2003 and references therein). This approach is based on the scavenging of particle-reactive ^{234}Th onto biogenic particles in the upper 100-200 m of the oceanic water column, followed by export of the ^{234}Th as the particles sink. The method usually involves measurement of particulate and dissolved ^{234}Th profiles in the water column. The flux of ^{234}Th required to support the deficit of this radionuclide in the water column is converted to a POC flux by multiplying the ^{234}Th flux by the POC/^{234}Th ratio on sinking particles. In most prior studies, water column ^{234}Th profiles were determined by sampling with in situ pumps or Niskin bottles, and the POC/^{234}Th on exported particles was taken to be that measured on the >53 μm or >70 μm particles filtered using in situ pumps (Buesseler et al., 1998, 2001; Cochran et al., 2000; Moran et al., 2003). While the "^{234}Th method" is straightforward in its application, numerous concerns have been identified regarding the details of converting a ^{234}Th deficit into a POC flux (e.g. Buesseler, 1991; Amiel et al., 2002; Cochran and Masqué, 2003; Moran et al., 2003; Savoye et al., 2006; Buesseler et al., 2006). Such issues include: steady-state vs. non-steady state interpretation of the water column ^{234}Th profiles, accurate estimation of the POC/^{234}Th ratio on sinking particles, and lack of agreement between water column-derived ^{234}Th (and concomitant POC fluxes) and those measured in sediment traps. Despite many applications of the ^{234}Th method, there have been relatively few comparisons of ^{234}Th deficits obtained from repeated sampling of ^{234}Th water column profiles with time-series sediment trap records of the ^{234}Th flux at the same station. Benitez-Nelson et

al. (2001) conducted such a study in the North Pacific and Gustafsson et al. (2004) compared detailed time-series water column ^{234}Th deficits with trap records of ^{234}Th flux in the Baltic Sea. Both studies compared the two sets of data with a perspective of "calibrating" the sediment trap fluxes with the water column ^{234}Th data.

The present paper is one of a series of three that address some of the issues mentioned above concerning the application of ^{234}Th as a proxy for POC flux. Stewart et al. (2007) compared water column ^{234}Th deficits (relative to ^{238}U) with ^{210}Po deficits (relative to ^{210}Pb) at the DYFAMED site (northwestern Mediterranean Sea; water depth ~2300 m) as indicators of POC flux. Stewart et el. (2007) also compared POC fluxes calculated from the radionuclide deficits using POC/^{234}Th (or POC/^{210}Po) ratios obtained from in situ filtration of particles vs. moored sediment traps. Szlosek et al. (this volume) consider the controls on POC/^{234}Th ratios in particles at the DYFAMED site separated according to settling velocity. Here we focus on temporal changes in water column ^{234}Th profiles and fluxes based on the integrated ^{234}Th deficiency in the upper water column at the DYFAMED site, as well as at a coastal site (depth ~370 m) in the northwestern Mediterranean Sea, and compare these fluxes with those recorded in sediment traps over the same time interval. Our goals are to compare the different measures of ^{234}Th flux and to consider discrepancies in the context of non-steady-state processes.

2. Methods

2.1. Sample Collection: Coastal site

Sampling occurred during the spring bloom in March-April, 1999 at a station (water depth 370 m) in the Mediterranean off Monaco (Fig. 1). All sampling was conducted within the area 43° 41.81' to 43° 41.90'N and 7° 26.60 to 7° 26.98'E. Three French-produced Technicap sediment traps were deployed at 170 m on separate moorings within a few hundred meters of one

another (Fig. 1). The traps, designated 3, 4 and 5 corresponded to Technicap models PPS-3, PPS-4 and PPS-5. Traps 3 and 4 were cylindro-conical, with collection areas of 0.125 m^2 and 0.05 m^2, respectively. Trap 5 was of conical design with a collection area of 1 m^2. Each trap contained a rotating sample carousel that collected one sample every two days. The traps were deployed for a 24-day period from March 11 to April 2, 1999. The trap cups were poisoned with buffered formalin.

Sampling in the water column occurred at approximately weekly intervals during sediment trap deployment. Due to wire limitations on the vessel used for water column sampling, only the upper 90 m was sampled. Deeper samples were collected during recovery of the traps at the end of the one-month deployment. Samples for ^{234}Th were collected using Challenger Oceanic battery-operated in situ pumps. Pumps were outfitted with prefilters including either a filter stack consisting of a 142 mm diameter Teflon mesh (70 μm) followed by a 142 mm diameter quartz microfiber filter (QM-A; 1 μm) or a single 293 mm diameter glass fiber GF/F filter (0.7 μm). Each pump included two Hytrex acrylic filter cartridges impregnated with manganese oxide to retain dissolved ^{234}Th (Livingston and Cochran, 1987). Profiles of temperature, salinity and fluorescence were obtained by CTD casts after collection of pump samples.

2.2. Sample Collection: DYFAMED site

As part of the MedFlux program, sampling was conducted in 2003 and 2005 at the French JGOFS time-series DYFAMED site (43° 25'N, 7° 52'E; water depth 2300 m) in the Mediterranean Sea, ~52 km off Nice (Fig. 1). A mooring that included an indented rotating sphere (IRS) time series sediment trap (Peterson et al., 1993) with a target depth of 200 m was deployed March 6, 2003, recovered in early May, and re-deployed until June 30. In 2005, the

trap was deployed from March 4 through April 28. Sample cups integrated the flux over 5-6 days during the first deployment and 4-5 days during the second deployment in 2003, and 5 days during the 2005 deployment. Actual depths of the traps, determined after recovery, were 238 m for March-May 2003, 117 m for May-June 2003 and 313 m for March-April 2005. The IRS traps exclude swimmers by collecting particles initially onto a rotating sphere with depressions that allow the particles but not macrozooplankton to sink into the carousel below the sphere (Peterson et al., 1993). All trap cups were poisoned with mercuric chloride.

Sampling in the water column occurred in March, May and June 2003 and March and April 2005; sampling depths are indicated in Table 1. Samples for ^{234}Th were collected using Challenger Oceanic battery-operated in situ pumps (2003 and 2005) and Niskin bottles deployed on a rosette (2005). In 2003, pumps were outfitted with prefilters including filter stacks consisting of a 142 mm diameter Teflon mesh (70 μm) followed by a 142 mm diameter quartz microfiber filter (QM-A; nominal 1 μm) or 293 mm diameter Nitex mesh (70 μm) followed by a glass fiber GF/F filter (0.7 μm). In 2005, all pumps used Teflon mesh and QM-A filters. Each pump included two Hytrex acrylic filter cartridges impregnated with manganese oxide to retain dissolved ^{234}Th (Livingston and Cochran, 1987). Pumps were operated for approximately 2 hours and filtered 500 – 1000 L. CTD casts were taken shortly before or after the pump casts for determination of hydrography.

2.3. ^{234}Th analysis

The Teflon prefilters from the in situ pumps were rinsed with filtered seawater to remove the particles, and were then re-filtered onto 25 mm QM-A filters and dried. The large diameter GF/F or QM-A filters from the pumps were dried and 21 mm punches were taken from the filter for ^{234}Th determination (equivalent to 48.8% of the 142 mm filter and 10.3% of the 293 mm

152 filter). The filters were placed in sample cups, either mounted singly in the case of the rinsed
153 Teflon screens or stacked in the case of multiple punches from the GF/F or QM-A filters. Splits
154 from the sediment trap cups were filtered onto 25 mm 0.4 μm Nuclepore filters, dried and
155 mounted on sample cups in the same geometry as the >70 μm particles from the pumps. The
156 cups were covered with plastic film and aluminum foil and beta counted at either the Stony
157 Brook University Marine Sciences Research Center (MSRC) or IAEA- Marine Environment
158 Laboratories (MEL) using Risø low background beta counters to measure the ^{234}Th activity
159 (Buesseler et al., 1998, 2001; Cochran et al., 2000). In a few cases, the rinsed Teflon filter was
160 sampled by taking punches and mounting them in a manner similar to the other samples. No
161 residual beta activity was detected above background, and we conclude that the rinsing
162 procedure was effective.

163 Samples were counted at least twice to a counting error of <5% to resolve ^{234}Th decay
164 and correct for any long-lived beta activity on the filters as well as the filter blank. All activities
165 were decay-corrected to the time of sample collection. The beta counting efficiency (0.41 for
166 single filters and 0.25 for stacked filters; precisions were approximately ±5%, depending on
167 laboratory) was determined by evaporating a small aliquot of ^{238}U standard in equilibrium with
168 ^{234}Th onto 21 mm filter punches and mounting the punches for counting in the same manner as
169 the samples. Generally, ^{234}Th activities in the >70 μm fraction were only a few percent of those
170 in the 1-70 μm fraction. Here we report the total particulate ^{234}Th (>1 μm). Details of the size-
171 fractionated ^{234}Th and the relationship between particulate ^{234}Th and POC are reported elsewhere
172 (Stewart et al., 2007; Szlosek et al., this volume).

173 The manganese cartridges were dried, ashed in a muffle furnace at 450° C and the ash
174 was then transferred into containers for counting. The ash was counted on intrinsic germanium

175 gamma detectors, and ^{234}Th was measured using its 63.3 keV gamma emission. Standards were
176 prepared by ashing cartridges that contained a known amount of ^{238}U in secular equilibrium with
177 ^{234}Th (Cochran et al., 1995; Rutgers van der Loeff et al., 2006). Manganese cartridge samples
178 collected in 2003 were counted either at IAEA-MEL or MSRC, whereas those collected in 2005
179 were all counted at MSRC. The counting procedure was slightly different in the two
180 laboratories: at IAEA-MEL, an aliquot comprising ~70% of the ashed cartridge was counted in a
181 well detector whereas at MSRC the entire ash was counted on a planar germanium detector.
182 Dissolved activities were determined based on the gamma activity on the first and second
183 manganese cartridges in series, using the method of Livingston and Cochran (1987). Errors
184 include counting errors and propagated errors on the counting efficiency.
185 Small-volume samples were collected from Niskin bottles in 2005 and total ^{234}Th was
186 determined using a modification of the method of Rutgers van der Loeff and Moore (1999) and
187 Buesseler et al. (2001). ^{230}Th was added as a yield tracer and Th was scavenged by precipitating
188 MnO_2 in the samples. The precipitate was filtered onto 25 mm diameter QM-A filters and
189 mounted for beta counting as described above. Samples were counted several times at the
190 Autonomous University of Barcelona to follow the decay of ^{234}Th. Subsequently they were
191 processed radiochemically (with the addition of ^{229}Th as a second yield tracer) to determine the
192 recovery of Th in the MnO_2 precipitate. The purified Th was electroplated and alpha counted,
193 obtaining recoveries that were generally >85%.
194 Cai et al. (2006) have recently questioned dissolved Th activities obtained by pumps.
195 Their analyses of 8 samples from the South China Sea showed offsets between pump and small
196 volume total ^{234}Th activities, as well as pump ^{234}Th activities that were less than the ^{238}U activity
197 in deep waters. Our 2005 data permit a comparison of the total ^{234}Th activities determined on

198 samples collected by both pump and Niskin bottle. We are also able to compare total ^{234}Th
199 activities in deep water with the ^{238}U activity. ^{238}U at the DYFAMED site was determined on 18
200 samples collected on March 13, 2005 over depths ranging from 25 to 2000 m. Samples were
201 analyzed at IAEA-MEL by sector field ICP-MS using isotope dilution with ^{236}U (Wyse et al.,
202 2006); values ranged from 2.68 – 2.72 dpm L^{-1} (mean ± 1σ = 2.70 ± 0.01 dpm L^{-1}). This value is
203 in agreement with that expected from the relationship between U and salinity obtained by Chen
204 et al. (1986), as re-interpreted by Pates and Muir (2007). The Chen et al. (1986) U/salinity
205 relationship (^{238}U = 2.458 dpm L^{-1} for 35‰ salinity; Pates and Muir, 2007) predicts ^{238}U
206 activities of 2.68 – 2.71 dpm L^{-1} for salinities observed at the DYFAMED site. Speicher et al.
207 (2006) used ICP-MS to determine ^{238}U values for the Ligurian, Tyrrhenian and Aegean Seas and
208 confirmed that the Chen et al.(1986) relationship between U and salinity held for these areas.
209 Pates and Muir (2007) made additional measurements of ^{238}U in the open Mediterranean and
210 suggested a U/salinity relationship slightly different from that of Chen et al. (1986) that yields
211 ^{238}U activities of 2.71 – 2.75 dpm L^{-1} for the DYFAMED site. In calculating ^{234}Th deficits at the
212 DYFAMED site, we use our directly measured ^{238}U value (2.70 dpm L^{-1}). Salinities were
213 slightly lower at the coastal site, and 2.65 dpm ^{238}U L^{-1}, obtained from the Chen et al. (1986)
214 U/salinity relationship, was used for calculating ^{234}Th deficits. The mean total ^{234}Th determined
215 at the DYFAMED site from pump samples >400 m in 2005 (n=8) depth is 2.59 ± 0.15 dpm L^{-1}.
216 The mean ^{234}Th determined on small volume samples >400 m depth (n=22) is comparable, 2.67
217 ± 0.14 dpm L^{-1}. Both are in agreement within the uncertainty with the ^{238}U activity.
218 We are also able to compare pump and small-volume total ^{234}Th on casts taken close in
219 time in 2005 (March 9 and March 13/14). The samples span depths from 5 to 1500 m and the
220 data scatter about a 1:1 line with no systematic offset (plot not shown). Pump and small-volume

221 ^{234}Th data from many locations (including the DYFAMED 2005 data) are compared by Hung et
222 al. (2008) and show no significant offsets. Hung et al. (2008) conclude that manganese oxide-
223 impregnated cartridges, when properly prepared and analyzed, yield reliable values for
224 "dissolved" Th in seawater. In particular, we strongly recommend that cartridges be ashed for
225 gamma spectrometric analysis of ^{234}Th. This method is preferable to wet chemical extraction
226 techniques (Cai et al., 2006) in that it ensures complete recovery of the Th retained on the
227 cartridge. This procedure also facilitates making a suitable standard, which is best prepared by
228 adding ^{234}Th in equilibrium with ^{238}U to a manganese oxide-impregnated cartridge and ashing
229 the cartridge.

230 **3. Results**

231 *3.1. Coastal site*

232 Figure 2a-c shows temperature, salinity and fluorescence profiles at four times
233 (approximately weekly) during the one-month trap deployment in 1999. Temperature was
234 relatively constant with depth during the first three weeks of sampling, increasing progressively
235 from March 11 until March 24 before showing a significant decrease from March 24 to March
236 31. Salinity decreased from March 11 to March 19, increased on March 24 and showed a
237 significant decrease in the upper 40 m between March 24 and March 31. Fluorescence profiles
238 were similar on March 11 and 31, with a maximum between 20-40 m. Fluorescence increased
239 throughout the upper 80 m between March 11 and March 19. Values from 50 – 80 m remained
240 high on March 24, but decreased in the upper 50 m.

241 Water column ^{234}Th profiles are shown in Fig. 3 (Table 1). Total particulate ^{234}Th
242 activities (>1 μm) were high (~0.3 – 0.4 dpm l^{-1}) in the March 11 and 19 profiles, and decreased
243 to <0.3 dpm l^{-1} in the profiles taken on March 24 and 31. Total ^{234}Th (particulate + dissolved)

244 was highest at the outset of sampling (Fig. 3a). A mid-depth minimum in total ^{234}Th, coincident
245 with the fluorescence maximum, was evident by the second sampling (Fig. 3b). Significant
246 water column deficits in ^{234}Th were evident in all four profiles; the deficits increased between
247 samplings on March 11 and 19, decreased between March 19 and 24, then increased again from
248 March 24 to 31 (Table 3). Data from sampling between 120 and 200 m at the end of the
249 sediment trap deployment (Table 1) suggest that deficits extended at least to 200 m at that time.
250 Although the fluxes of ^{234}Th recorded in the three sediment traps often agreed quite
251 closely, at times they differed by a factor of 2 (Table 2). No systematic offset was observed,
252 such that the flux recorded in one type of trap was consistently greater or less than another. For
253 purposes of comparing the trap and water column data (see below), we use the average flux from
254 the three traps at any given time. The time series record of average fluxes shows that values are
255 relatively constant over the first ~3 weeks, 3070 ± 700 dpm m^{-2} d^{-1} from March 11-29, but
256 decreased progressively to ~600 dpm m^{-2} d^{-1} from March 29 to April 2.
257 *3.2. DYFAMED site*
258 The hydrography of the DYFAMED site during the time of our sampling in 2003 has
259 been discussed in detail by Stewart et al. (2007). Important water masses in the upper few
260 hundred meters include surface water (Modified Atlantic Water, MAW) and Levantine
261 Intermediate Water (LIW). In addition, Winter Intermediate Water (WIW) can be formed in the
262 winter and spring by cooling of surface water by northwesterly winds (Fieux, 1974; Conan and
263 Millot, 1995; Millot, 1999). WIW is displaced below MAW after cessation of the winds. T-S
264 diagrams show the presence of WIW at ~60 m in early March 2003. In 2005, detailed
265 hydrographic data are available only during the trap deployment cruise in March. A strong
266 increase in salinity (and σ_t) is evident in the upper 200 m, occurring between March 11 and

13/14 (Fig. 4a). Increases in fluorescence are also evident on March 14, relative to the preceding period (March 8-13; Fig. 4b).

The water column ^{234}Th profiles (Table 1; Figs. 5-6) generally show deficits of ^{234}Th relative to ^{238}U in the upper 100 m at all sampling times in 2003 and 2005. In 2003, total particulate ^{234}Th activities (>1 μm) were greatest during the June sampling, and in the May and June profiles, displayed a maximum at ~50 m. This maximum was coincident with the fluorescence (chlorophyll a) maximum. In 2005, particulate Th data are available only from the pump casts on March 9 and 13. The March 13 profile shows a distinct particulate ^{234}Th maximum at ~25 m, also coincident with the pronounced maxima in the fluorescence profiles that developed March 13/14 (Fig. 4b).

Data on composition of the trap material and fluxes of mass, POC and major components ($CaCO_3$, biogenic silica, lithogenic material) in IRS traps deployed in 2003 and 2005 are given elsewhere (Lee et al., this volume). During the first trap deployment in 2003 (March-May, 238 m), maximum fluxes of ^{234}Th (~2300 dpm m^{-2} d^{-1}; Table 2), as well as mass and particulate organic carbon, occurred in early March. These corresponded to high fluxes of diatom aggregates and zooplankton fecal pellets (Lee et al., this volume; Wakeham et al., this volume). ^{234}Th fluxes decreased in late March to about 25% of the maximum values and remained at that level until early May, when the trap was recovered. At the beginning of the second deployment (May-June, 117 m), ^{234}Th fluxes were ~500 dpm m^{-2} d^{-1} and decreased to low values (~10 dpm m^{-2} d^{-1}) by June. This latter period included bacterially degraded phytoplankton cells. (Wakeham et al., this volume) No flux data are available for early May while the trap mooring was being recovered and re-deployed.

289 In 2005 the shallow IRS trap was deployed at 313 m for only ~2 months (March-April).
290 The pattern of ^{234}Th fluxes was somewhat different than in 2003, with maxima (~2500 dpm m^{-2}
291 d^{-1}) in both early and late March (Table 2). Fluxes dropped to values of ~70 dpm m^{-2} d^{-1} by late
292 April. Such low fluxes were not evident until June in 2003, but the different timing of bloom
293 and dust events (Lee et al., this volume), as well as different trap deployment depths, in 2003 and
294 2005 make it difficult to compare the records rigorously.
295
296 **4. Discussion**
297 *4.1. Estimating ^{234}Th fluxes*
298 Application of ^{234}Th-^{238}U disequilibrium in the water column for estimating POC fluxes
299 requires determining the ^{234}Th deficit, and logistical constraints on ship time frequently result in
300 the deficit being determined from a single water column profile at a station. Conversion of the
301 ^{234}Th deficit into a reliable local ^{234}Th flux involves an understanding of the extent to which the
302 ^{234}Th profile is in steady state and is dominated by local processes (e.g. uptake onto particles
303 produced and sinking locally), information that is often lacking. Here we are able to compare
304 ^{234}Th fluxes suggested by water column ^{234}Th deficits and those measured in sediment traps at
305 the same time.
306 The time-rate-of-change of ^{234}Th in the water column is given by
307
308 $$\frac{\partial A_{Th}}{\partial t} = \lambda_{Th} A_U - \lambda_{Th} A_{Th} - F_{Th} + V \qquad (1)$$
309
310 where A_U and A_{Th} are the ^{238}U and total (particulate + dissolved) ^{234}Th activities

311 (dpm m^{-2}), respectively, integrated over some depth z, λ_{Th} is the ^{234}Th decay constant, F_{Th} is the
312 flux of total ^{234}Th through depth z (dpm m^{-2} d^{-1}) and V is the sum of advective and diffusive
313 transport.

314 A common approach to calculating ^{234}Th fluxes from water column deficits is to assume
315 steady state ($\partial A_{Th}/\partial t = 0$) and negligible V, in which case the ^{234}Th flux is

316

317 $$F_{Th} = \lambda_{Th} D \quad (2)$$

318

319 where D is the water column ^{234}Th deficit (dpm m^{-2}) between depths $z = 0$ and $z = z_{max}$,
320 defined as

321

322 $$D = \int_0^{z_{max}} [A_U - A_{Th}(z)]dz \quad (3)$$

323

324 ^{234}Th deficits (Table 3) for each profile were calculated using trapezoidal integration and
325 propagation of measurement errors (Rutgers van der Loeff et al., 2006). In practical terms, the
326 integration uses the difference between the ^{238}U activity and measured ^{234}Th activity (dpm m^{-3} at
327 any given depth z integrated over the depth interval (m) spanning the mean distance between
328 depths z and z-z_u and z and z+z_l (where z_u and z_l represent the sampling depths above and below
329 z, respectively). Integration of the Th water column deficits at the DYFAMED site was done to
330 depths corresponding most closely to the sediment trap deployments: 200 m for March-May,
331 2003, 100 m in May-June, 2003 and 300 m in March-April, 2005 (Table 3). For the coastal site,
332 ^{234}Th was integrated over the depth of the water column profile (90 m).

333 For a flux regime such as a bloom, in which the Th flux may be expected to be low
334 initially, increase with time and then decrease, the water column ^{234}Th deficit will track the flux

such that deficits will increase and decrease. Under such conditions, and assuming no horizontal advection, the rate of change of D may be expressed as

$$\frac{dD}{dt} = -\lambda_{Th} D + F(t) \qquad (4)$$

where $F(t)$ is the flux of ^{234}Th activity (dpm m^{-2} d^{-1}) through the surface $z = z_{max}$.

Equation (4) illustrates the fact that while there may be large short-term changes in Th flux, the water column Th deficit has a "memory" of previous scavenging events that produced a deficit (D in Eq. 4). The decay term $(-\lambda_{Th}D)$ in Eq. (4) effectively serves to smooth out the variation in water column deficit relative to the pattern of flux recorded in a trap. This observation can be demonstrated by a thought experiment in which the sinking flux of ^{234}Th is initially high, such as during or immediately after a bloom, then is rapidly reduced to zero as the bloom subsides. The water column ^{234}Th deficit caused by this flux will not decrease immediately, but instead will decrease at a rate determined by the half-life of ^{234}Th as it grows toward equilibrium with ^{238}U. Indeed, this idea was expressed by Ku and Musakabe (1990) in their analysis of the bias introduced into estimations of apparent mean residence time with respect to scavenging for natural radionuclides of differing half-life after a transient removal of one-half of the radionuclide inventory from surface water. We can test this idea with the present data by solving Eq. (4) for the ^{234}Th deficit, and then use the high-temporal resolution record of ^{234}Th fluxes recorded in the trap to determine whether the pattern of observed water column deficits is consistent with that expected from the trap flux. Integrating Eq. (4) produces the non-steady state prediction of the change in ^{234}Th deficit with time:

$$D(t_0 + T) = D(t_0)e^{-\lambda_{Th}T} + \int_{t_0}^{t_0+T} e^{\lambda_{Th}(t_0+T-t)} F(t)dt \qquad (5)$$

where t_0 is the starting time of the integration interval and *T* is its duration. Here the first term on the right hand side reflects decay of the ^{234}Th deficit present at t_0, and the second term is the introduction of new deficit through thorium export, weighted for decay between export at time *t* and the end of the interval at $t_0 + T$. In applying Eq. (5) to data, we assume that the ^{238}U activity is constant with time. Given the relatively small range in salinity observed with time at the DYFAMED site, this assumption is reasonable. Indeed, as the estimates of dissolved ^{238}U cited in section 2.3 suggest, ^{238}U is expected to vary by ~1% for the range of salinities observed.

A piecewise solution for Eq. (5) can be obtained by assuming that flux F_i is constant between two successive times t_i and t_{i+1} in a flux record (e.g. midpoints of collection for two adjacent trap cups):

$$D(t_{i+1}) = D(t_i)e^{-\lambda_{Th}(t_{i+1}-t_i)} + (F_i / \lambda_{Th})(1 - e^{-\lambda_{Th}(t_{i+1}-t_i)}) \quad (6)$$

Eq (6) is then used to produce the deficit estimates used in Figs. 7, 9, and 11. Eq. (6) can also be inverted to give estimated fluxes $\hat{F}_i$ for each time interval:

$$\hat{F}_i = \lambda_{Th} \frac{D(t_{i+1}) - D(t_i)e^{-\lambda_{Th}(t_{i+1}-t_i)}}{1 - e^{-\lambda_{Th}(t_{i+1}-t_i)}} \; ; \quad (7)$$

Eq. (7) is used to produce the flux estimates in Figs. 8, 10, and 12.

Eq. (7) is effectively that developed by Buesseler et al. (1992) to estimate non-steady fluxes from water column ^{234}Th deficits that were changing with time. However, the time interval $t_{i+1} - t_i$ in the case of Buesseler et al. (1992) and others who have used this formulation (see Savoye et al., 2006) was of the order 1-4 weeks, much longer than the temporal resolution

379 afforded by traps in our experimental settings. In contrast, our sediment trap data provide a
380 detailed temporal record (over 2-5 day intervals) of the ^{234}Th flux, *F* in Eqs. (5) and (6), at the
381 coastal site and DYFAMED site. We use this record in Eq. (6) to predict the ^{234}Th deficit that
382 should be observed in the water column above the trap depth, under the assumption that the
383 observed deficit is produced locally by scavenging of ^{234}Th onto sinking particles caught in the
384 trap. Any differences between the water column deficit implied by the trap fluxes (using Eq. 6)
385 and measure water column deficits must then be explained by factors such as trapping efficiency
386 or advective influences on dissolved and particulate ^{234}Th, as discussed below.

387 For each time point *i*, we calculated the likelihood component $L_i(t_i)$, the probability that
388 the measured water column ^{234}Th deficit *i* could have been produced by Eq. (8) using a given set
389 of parameters (see below):

390

391 $$L_i(t_i) = \frac{1}{\sqrt{2\pi\sigma_i^2}} \exp\left(- \frac{(D_i(t_i) - \hat{D}(t_i))^2}{2\sigma_i^2} \right) \quad (8)$$

392

393 (Edwards 1992; Hilborn and Mangel 1997). Here $D_i(t_i)$ is the measured water column ^{234}Th
394 deficit at time t_i, and $\hat{D}_i(t_i)$ is the prediction of $D_i(t_i)$ that is implied by the trap fluxes (Eq. 6)
395 Eq. (8) also reflects the assumption that errors are distributed normally with variance σ_i^2; this
396 variance is calculated for each water column ^{234}Th deficit *i* as the sum of a the estimated
397 measurement error of $\mathrm{var}(D_i(t_i))$ and an (assumed constant) "environmental variance" σ_{env}^2 that
398 accounts for other "error-producing" processes, such as small-scale and mesoscale advection,:

399

400 $$\sigma_i^2 \equiv \mathrm{var}(D_i(t_i)) + \sigma_{env}^2 \quad (9)$$

401

402 Estimating $\hat{D}_i(t_i)$ required estimating three parameters: an initial deficit $\hat{D}(0)$; an

403 environmental variance σ^2_{env}; and a constant multiplier α to account for possible biases in trap

404 collection efficiency. The equations used were

405

406 $$\hat{D}_j(t_j) = \hat{D}(0) + \alpha \sum_{t_i=0}^{t_{i+1}=t_j} \Delta\hat{D}(t_i, t_{i+1}) \quad (10)$$

407 and, from Eq. (6),

408

409 $$\Delta\hat{D}(t_i, t_{i+1}) \equiv \hat{D}_{i+1}(t_{i+1}) - \hat{D}_i(t_i). \quad (11)$$

410 Finally the likelihoods for the individual water column measurements (Eq. 8) are

411 combined as

412 $$L = \prod_{i=1}^{n} L_i \quad (12)$$

413 and the parameters $\hat{D}(0)$, σ^2_{env}, and α are estimated using a program that finds the values of

414 those parameters that maximize the value of L in Eq. 12 (see, e.g., Metropolis et al., 1953; Hurtt

415 and Armstrong, 1994).

416 One point deserves special attention: the requirement that the initial condition $\hat{D}(0)$ and

417 α must be estimated makes the mean estimate of the deficit derived using Eqs. (10) and (11)

418 track the average of measured water column deficits. This fact in turn implies that the

419 comparison of the two estimates is made by comparing their time-evolution, not their mean

420 values.

421 *4.2. Comparing traps and water column ^{234}Th deficits and fluxes: coastal site*

422 Figure 7 shows the water column ^{234}Th deficits, $\hat{D}_i(t_i)$, predicted from the trap flux record

423 at 170 m over the ~1 month deployment (dashed line), calculated using Eq. (6). The measured

424 water column Th deficits (0-90 m), $D_i(t_i)$, at the four sampling times are shown for comparison.
425 Although the traps were deeper than the depth of integration for the water column Th profiles,
426 the measured deficits bracket those predicted from the trap fluxes, with the first and third
427 measurements lying below, and the second and fourth lying above, the trap-predicted values.
428 The pattern of predictions of $\hat{D}_i(t_i)$devolves directly from the trap record, which shows little
429 change in flux for approximately three weeks, then a decline in the fourth week. The predicted
430 water column ^{234}Th deficit increases slightly during the first three weeks of the record, under
431 conditions of relatively constant ^{234}Th flux (Table 2; Fig. 7). As expected, the predicted water
432 column ^{234}Th deficit toward the end of the record changes more slowly with time than the trap
433 flux because of the effective lag produced by the radioactive mean-life of ^{234}Th ($1/\lambda_{Th}$ or 34.8
434 days). Therefore, although the trap Th flux decreases by ~80% during the last 4 days of sampling
435 (Table 2), the predicted water column deficit decreases only slightly in this interval (Fig. 7).
436 Under conditions of low or zero ^{234}Th flux (F(t) = 0 in Eqs. 5 and 6), the deficit would continue
437 to decrease, approaching zero as ^{234}Th approaches equilibrium with ^{238}U.

438 The water column ^{234}Th deficits are generally consistent with the trap record in this
439 instance. Indeed, Fig. 8 shows that steady-state ^{234}Th fluxes calculated from the water column
440 deficits (Eq. 2) agree well with trap fluxes for the first three profiles. However, the deficits do
441 vary significantly from one profile to the next (Table 3). Figure 8 shows the effect of these
442 variations on non-steady state fluxes of Th calculated using Eq. (7), where the times t_i and t_{i+1}
443 are times of water column sampling. The non-steady- state fluxes predicted from the change in
444 deficit between March 11 and 18 and especially between March 18 and 24, diverge strongly from
445 the trap record. In particular, the decrease in deficit between the March 18 and 24 profiles
446 requires a negative ^{234}Th flux (i. e., addition of ^{234}Th to the water column). Such a pattern

447 demonstrates the sensitivity of calculations made using Eq. (7) to relatively small variations in
448 deficit, especially when water column profiles are taken closely in time. This sensitivity was
449 pointed out by Savoye et al. (2006) in their review of approaches to reconstructing non-steady
450 state ^{234}Th fluxes from water column ^{234}Th deficits.

451 An additional factor may be advective influences on the profiles. The hydrography (Fig.
452 4) shows significant increases in T and S and decreases in fluorescence between March 18 and
453 24 that depart from the sequence of changes resulting from seasonal temperature variation and
454 progression of the spring bloom, as indicated by T, S and fluorescence data at the other three
455 sampling times. Finally, the water column ^{234}Th profiles include only the upper 90 m of the
456 water column while traps were deployed at 170 m. Although ^{234}Th deficiencies are frequently
457 greatest in the upper ~100 m, there may be deficits at greater depths. Water samples taken at
458 100-200 m on April 7, 1999 suggest that the deficit extended deeper than 90 m at that time
459 (Table 1). If the temporal change in deficit from 90 – 170 m tracked that in 0-90 m, the general
460 agreement between the observed and predicted pattern of increasing ^{234}Th deficits in response to
461 a sustained and nearly constant flux of ^{234}Th as recorded in the traps still obtains. However, the
462 ^{234}Th flux recorded by the traps would be less than that predicted from the deficits, on average.
463 This may be due to a trapping efficiency that is constant with time but less than 100%. The
464 general similarity of fluxes recorded by three very different trap designs makes this seem
465 unlikely, but it is difficult to fully assess this possibility without more complete sampling of the
466 water column. This emphasizes the importance of determining deficits to the same depth at
467 which trap fluxes are measured for optimum comparison of the two estimates of ^{234}Th flux.
468 Sampling at the DYFAMED site was designed with this strategy in mind.

469 *4.3. Comparing traps and water column ^{234}Th deficits and fluxes: DYFAMED site*

Measured ^{234}Th deficits at the DYFAMED site in 2003 increase from early March to higher values in May and June (Fig. 9). As noted earlier, the sediment trap fluxes are highest in early to mid- March, during the first trap deployment (at 238 m), with values decreasing sharply until early May (Table 2; Fig. 10). The second deployment in 2003 (at 117 m) shows fluxes in May comparable to those at the end of the first deployment, decreasing to low values by late June (Table 2; Fig. 10). It is not possible to use Eq. (6) directly to predict the water column ^{234}Th deficits that are consistent with the trap fluxes throughout the entire ~4 months of the trap record because the depth of trap deployment changed between deployments. The offset in the trap-predicted curves of ^{234}Th deficit with time in Fig. 9 is produced by scaling the values in the second deployment to the mean ratio (~0.6; Table 3) of the Th deficit in the upper 100 m to that in the upper 200 m in early May, when the trap turnaround occurred. The lower curve in Fig. 9 is the best fit obtained by fitting the trap fluxes to observed water column deficits; the upper curve is a best fit obtained by adding a constant scaling factor (α in Eq. 10) to the trap record. The latter (with a scaling factor of 2.1) fits the water-column ^{234}Th deficits significantly better, because its log(likelihood) is more than two units greater than the curve obtained without scaling. In effect this scaling assumes that the trapping efficiency is ~50%, and in this case the water column ^{234}Th deficit in March and in early May lie on the curve. Neither predicted curve reproduces the high ^{234}Th deficit in late June. Indeed, trap ^{234}Th fluxes had dropped to near zero by that time and, even allowing for the temporal lag in variation in the water column deficit produced by the 34.8-day mean life of ^{234}Th, the trap record predicts low water column deficits ($<1 \times 10^4$ dpm m^{-2}) by late June.

Another feature of the measured water column ^{234}Th deficits evident in Fig. 9 is the temporal variability over a few days in early May. Values (0-200 m) vary from 3.9×10^4 to $5.6 \times$

493 10^4 dpm m^{-2}, but do overlap within errors. Stewart et al. (2007) examined this time interval in
494 detail in the context of comparing $^{234}Th/^{238}U$ and $^{210}Po/^{210}Pb$ estimations of POC flux. They
495 observed considerable variability in surface chlorophyll as indicated by satellite observations. In
496 particular, satellite data showed a shift from low temperature-high chlorophyll surface water on
497 May 7 to higher temperature-lower chlorophyll water on May 8 which persisted until May 13.
498 While the satellite data are representative only of surface water, this pattern corresponds closely
499 to the decrease in Th deficit from high values on May 7 to lower values on May 11 and 13.

500 Steady-state ^{234}Th fluxes calculated from measured water column ^{234}Th deficits using Eq.
501 (2) also do not correspond well to the fluxes recorded in the traps (Fig. 10); deficit-derived fluxes
502 are lower than the trap fluxes by a factor of ~3 for the March water column deficit, are greater by
503 a factor of ~3 for the May profiles and are greater by a factor of ~150 in June. In addition, the
504 time between measured ^{234}Th profiles is generally long (except in early May, when it is only a
505 few days) so that the non-steady state fluxes calculated from the water column ^{234}Th deficits (Eq.
506 7; shown as horizontal dashed lines in Fig. 10) are essentially those given by the second profile
507 for any given pair of profiles. That is, Eq. 7 reduces to the steady-state estimation of flux from
508 the deficit at time = $t + 1$, $\hat{F}_i \approx \lambda D(t_{i+1})$, because the time difference between water column
509 profiles (t_{i+1} - t_i) is long relative to $1/\lambda_{Th}$. We have not attempted to calculate non-steady state
510 fluxes for the short-term variation in water column deficits in early May because of the short
511 times between profiles and the consequent large errors (Savoye et al., 2006).

512 The 2005 data show a similar discrepancy between the pattern of trap ^{234}Th fluxes and
513 water column deficits (Figs. 11 and 12). Deficits (calculated to 300 m to match the trap depth)
514 increased from the March 2 profile (2.4 x 10^4 dpm m^{-2}) to the deficits indicated by the small-
515 volume and pump-derived profiles on March 9 (9.3 x 10^4 dpm m^{-2} and 6.7 x 10^4 dpm m^{-2},

516 respectively; Fig. 11). Deficits ranged by a factor of 7 over the five days of sampling between
517 March 9 and March 14, and then dropped to low values on April 29. Indeed the deficit was
518 negative on April 29, largely due to surpluses of ^{234}Th relative to ^{238}U in the 200-300 m depth
519 interval (Fig. 6g). We note that these surpluses do not simply balance the Th deficit in the upper
520 200 m, as might be expected if remineralization of settling particles released the associated ^{234}Th.
521 Instead, the net surplus implies addition of ^{234}Th to the upper 300 m in excess of local production
522 from ^{238}U.

523 Sediment trap fluxes in 2005 do show a minimum on March 16, with maxima on March 6
524 near the beginning of the trap deployment and on March 31 (Table 2; Fig. 12). If the water
525 column deficit is produced locally by ^{234}Th fluxes as recorded in the trap, the best-fit pattern of
526 the deficits consistent with the trap record is shown in Fig. 11. As with the 2003 data, few of the
527 observed water column deficits lie on the trend defined by the trap flux record (Fig. 11) and,
528 unlike 2003, no scaling of trap fluxes produces a better fit. In particular, the substantial ^{234}Th
529 fluxes recorded in the traps throughout March (875 – 2500 dpm m^{-2} d^{-1}) should leave a "residual"
530 ^{234}Th deficit in the water column at the end of April (approximately one ^{234}Th half-life later).
531 Instead, the water column Th deficit is negative at the end of April, indicating supply of ^{234}Th
532 above local production from ^{238}U to the area. Steady-state ^{234}Th fluxes (Eq. 2) calculated from
533 the water column deficits do overlap the trap fluxes on March 9 and 13/14 but are divergent on
534 other dates (Fig. 12).

535 The sinking flux of POC is often estimated from the ^{234}Th deficit in the upper water
536 column by multiplying the steady-state ^{234}Th flux obtained from the deficit by the POC/^{234}Th
537 ratio of large filterable particles (e.g. Buesseler et al., 1998, 2006; Moran et al., 2003; see also
538 Cochran and Masqué, 2003) . Stewart et al. (2007) have shown that when this approach is taken

539 with the 2003 DYFAMED water column data, the POC fluxes calculated from water column
540 ^{234}Th deficits are generally greater than those measured in the IRS time-series sediment traps.
541 *4.4. Effects of trapping efficiency on ^{234}Th fluxes recorded by traps*
542 Sediment trap design (surface area, aspect ratio) and hydrodynamic effects (current flow
543 regime in which traps are emplaced) can affect the efficiency with which traps collect settling
544 particles (Gardner, 1980; Baker et al., 1988; Gust et al., 1996; Gust and Kozerski, 2000; see also
545 the extensive review by Buesseler et al., 2007) and produce biases (positive or negative) in trap
546 ^{234}Th fluxes relative to those calculated from water column deficits (Buesseler, 1991). Our data
547 were collected using several trap designs. At the coastal site, three different traps were used,
548 with different surface areas and aspect ratios, yet Table 2 shows that there is no systematic
549 difference among the traps. Traps 3 and 4 differ in surface area by a factor of ~2, and trap 5 has
550 a collection area 8x and 20x those of traps 3 and 4, respectively. Yet the trap ^{234}Th fluxes
551 commonly agree to within 25 – 30%.
552 One factor that may affect trapping efficiency is the current regime to which the traps are
553 exposed. Current meter records obtained from the coastal site moorings with traps 3 and 5
554 showed current velocities ranging from 5 to 20 cm s^{-1} and had comparable temporal patterns at
555 the two sites. Current direction was mostly from the southwest, with highest velocities during
556 the interval March 22 – 28, 1999. Weaker flows from the northeast occurred in the intervals
557 March 14 –16 and March 30 – April 2, 1999. There is a suggestion in the data (e.g., greater
558 standard deviation of the mean flux on March 25) that agreement among the traps was poorer
559 than average in the interval with strong currents from the southwest (March 22 – 28), but it is
560 difficult to determine if this was systematic. With respect to comparison of ^{234}Th deficits
561 obtained from trap fluxes and water column Th profiles, there is no sense of a systematic bias

562 (Fig. 7), although as noted above the different depths of water column sampling (0 - 90 m) and
563 trap deployment (170 m) make it difficult to rigorously compare the two estimates of flux..
564 At the DYFAMED site, current velocities for the shallow trap (~200 m) ranged from 2 -
565 29 cm s^{-1} (mean 4.6 cm s^{-1}) in March-May and 1 - 13 cm s^{-1} (mean 4.5 cm s^{-1}) in May-July,
566 2003. In February-April, 2005, velocities ranged from 0.5 – 27 cm s^{-1} (mean 12 cm s^{-1}). The IRS
567 trap deployed at the DYFAMED site was designed to prevent collection of swimmers (Peterson
568 et al., 1993). At the same time as the MedFlux trap deployment, a Technicap PPS-5 was
569 deployed as part of the long-term DYFAMED time-series program. This trap showed lower
570 fluxes, but the same temporal pattern, as recorded in the MedFlux IRS trap. The difference in
571 fluxes recorded in the two traps suggests that significant spatial differences in flux exist, even on
572 a scale of a few km, or that trapping efficiencies are different for the two trap types.
573 Buesseler et al. (2007) have summarized several studies that compared long term trap
574 records with fluxes determined from water column ^{234}Th deficits and concluded that there is an
575 undertrapping bias of approximately a factor of 2 on average. At the deep-water JGOFS time
576 series sites HOTS and BATS, fluxes calculated from water column ^{234}Th profiles have been
577 compared with short-term floating trap deployments (Benitez-Nelson et al. 2001, Buesseler et al.
578 2000,) and the trap fluxes were found to be lower on average than those estimated from a steady-
579 state model applied to the deficits. Because the trap fluxes at each site were not continuously
580 recorded, however, part of the disagreement may have been due to the possibility that high flux
581 events were not sampled by the traps (Benitez-Nelson et al. 2001). Moreover, Buesseler et al.
582 (2000) noted that trap fluxes seemed to be lower than those predicted from the water column
583 ^{234}Th deficits during times of high flux and greater than predicted during periods of low flux.
584 Gustafsson et al. (2004) extended this idea by proposing that seasonal changes in trapping

585 efficiency are related to the settling velocities of the particles, such that fluxes predicted from
586 water column ^{234}Th deficits agree better with traps when the flux is dominated by rapidly settling
587 material (e.g. diatoms).

588 We are able to test some of these ideas with the MedFlux data from the DYFAMED site.
589 Scaling the trap fluxes by a factor of 2 for the 2003 data does result in a significantly better
590 agreement between trap and water column-derived estimates of ^{234}Th deficits (Fig. 9). This may
591 be interpreted as corresponding to a trapping efficiency of 50%. However, such scaling helps to
592 fit the high ^{234}Th deficits in early May, but fails to explain the continued high water column
593 deficit at the end of June (Fig. 9), a time at which the Mediterranean has become more
594 oligotrophic and fluxes are low. For the 2005 data, no scaling of trap fluxes produces a
595 significantly better fit of trap-derived ^{234}Th deficits to the water column data (Fig. 11).

596 Simultaneously with the time-series traps and at the same depths, IRS traps were
597 deployed and operated in a mode that sorted particles according to settling velocity (SV;
598 Peterson et al. 2005, this volume; Armstrong et al., this volume; Xue and Armstrong, this
599 volume; Lee et al., this volume). The ^{234}Th data from the SV traps are discussed in detail by
600 Szlosek et al. (this volume). The SV traps show that most of the ^{234}Th (and mass) flux is
601 contributed by particles settling at rates >200 m d^{-1}, comprised of zooplankton fecal pellets and
602 enriched in the ballast minerals calcium carbonate and biogenic silica. As summertime
603 oligotrophic conditions developed in 2003, increases were evident in the proportion of slowly
604 settling material comprising bacterially degraded phytoplankton cells, and the rapidly settling
605 material was dominated by calcium carbonate (Lee et al., this volume; Wakeham et al., this
606 volume). This period of low trap flux shows the greatest discrepancy with the water column
607 ^{234}Th deficit (Fig. 9), in contrast with the observations of Buesseler et al. (2000). Although one

608 could argue that a greater fraction of the settling material later in the season was slowly settling,
609 bacterially-degraded phytoplankton cells and that this material was undercollected by the traps,
610 the oligotrophic nature of the northwest Mediterranean in the summer suggests that the settling
611 particles fluxes are indeed low at that time and that the water column ^{234}Th deficit measured in
612 2003 does not accurately reflect local Th scavenging and flux. Moreover the long-term sediment
613 trap record (regardless of trap type) at the DYFAMED site is consistent with the seasonal nature
614 of production and flux in the northwest Mediterranean (Miquel et al., 1994; Miquel and LaRosa,
615 1999). We emphasize that the pattern of water column ^{234}Th deficits poorly matches the non-
616 steady state pattern predicted from the trap record in both 2003 and 2005 (Figs. 9 and 11) and
617 next consider constraints on the interpretation of water column ^{234}Th profiles as an indicator of
618 the local settling flux of ^{234}Th.

619 *4.5. Advective effects on water column ^{234}Th profiles*

620 Advection, both lateral and vertical, can influence particulate fluxes and water column
621 profiles of ^{234}Th (as well as those of many other reactive chemical species in the oceans).
622 Sediment traps, by definition, catch the sinking particulate flux of ^{234}Th. In contrast, water
623 column ^{234}Th deficits provide an indirect measure of the ^{234}Th flux on settling particles.
624 Significantly, the ^{234}Th deficit is dominated by the "dissolved" ^{234}Th fraction because, despite
625 high particle reactivity, more ^{234}Th is in solution than on particles at particle concentrations
626 typical of the open ocean (e.g., Table 1). This distinction provides a means for decoupling the
627 flux of ^{234}Th measured in a trap and estimated from a water column ^{234}Th profile. The fact that
628 mass and ^{234}Th fluxes collected in the settling velocity traps were dominated by particles settling
629 at rates >200 m d^{-1} (Armstrong et al., this volume,; Szlosek et al. this volume) implies that
630 particles (or mass and associated ^{234}Th) are transferred from the surface to the shallow traps

631 considered here (117 – 313 m) on time scales of the order of 1 day. Current speeds as high as 15
632 and ~30 cm s^{-1} were observed on our MedFlux moorings at the DYFAMED site in 2003 and
633 2005, respectively (M. Peterson, Univ. of Washington). For current velocities of 5 - 20 cm s^{-1},
634 settling particles might be transported distances of 4 - 17 km before they are caught in a trap
635 deployed at ~200 m. This is the effective size of the "statistical funnel" or area over which a trap
636 can integrate the particle flux (Siegel et al., 1990; Siegel and Deuser, 1997). In contrast,
637 dissolved ^{234}Th is advected over distances determined by its radioactive mean-life ($1/\lambda_{Th}$ or 34.8
638 d) and can be produced by decay of ^{238}U, scavenged, or recycled en route. Over one mean-life,
639 dissolved ^{234}Th can be transported ~170 - 650 km at flow velocities of 5 - 20 cm s^{-1}. In effect,
640 the water column ^{234}Th deficit is integrating water column processes (i. e., scavenging) over
641 distance scales ~40x those of a sediment trap. As noted above there is evidence from
642 hydrographic data at both coastal and DYFAMED sites and satellite data at DYFAMED of short
643 term variations in water mass structure. Such variations would likely have a greater impact on
644 dissolved ^{234}Th and the water column ^{234}Th deficit than on particle fluxes.
645 Indeed, the ^{234}Th deficits in the spring, 1999 (0-90 m) at our coastal site are
646 approximately three times greater than those observed in the upper 100 m at the DYFAMED site
647 in early March 2003 (Table 3). If the patterns seen in the two years are comparable and a water
648 mass with a deficit typical of the coastal site was advected to the DYFAMED site at speeds of 5
649 cm s^{-1} with no additional scavenging, it would be reduced to 30% of its initial value via ingrowth
650 over a time scale of ~40 d and a distance of ~150 km. The DYFAMED site is only ~50 km from
651 shore, and such a calculation demonstrates that advective transport can account for the deficit
652 observed at the DYFAMED site. However, it does not take into account the actual flow path of

653 the water or the fact that the site is generally considered to be isolated from advective input of
654 coastal waters by the westward flowing Northern Current (Bethoux et al. 1998; Millot, 1999),
655 Stewart et al. (2007) documented that the DYFAMED site showed several types of
656 advective influences during early 2003. For example, T-S diagrams show that the Mediterranean
657 surface water (Modified Atlantic Water, MAW) is underlain by another water mass, Winter
658 Intermediate Water (WIW) at ~60 m in March-April, 2003. WIW can form in the shelf area of
659 the northwestern Mediterranean (Fieux, 1974) and may have lower ^{234}Th activities, much as was
660 observed at our coastal site, as a consequence of the greater scavenging there. Advective effects
661 in surface waters may be important as well. For example, as noted above, satellite observations
662 document significant short-term (i. e., over a few days) changes in near-surface properties in
663 early May, 2003 (Stewart et al., 2007). For example, a patch of high Chl a was observed on May
664 7, but not on subsequent days. This was accompanied by high temperatures and a greater ^{234}Th
665 deficit than observed just a few days later on May 10/11 and 13.
666 In 2005, the variation in ^{234}Th deficit observed between March 9 and 14, 2005, in
667 particular the decrease in deficit from values of 7.5 – 14.1 x 10^4 dpm m^{-2} on March 9-11 to lower
668 values (2.2 - 4.6 x 10^4 dpm m^{-2}) on March 13-14, coincides with increases in salinity and
669 fluorescence in the upper 200 m over the same time (Fig. 4). Indeed, low deficits seem to follow
670 strong wind events. Sustained winds of 20-36 knots occurred from February 27 to March 1,
671 preceding the first water column ^{234}Th profile (March 2). A similar interval of strong winds (20-
672 38 knots sustained) occurred from March 12 to 13. Both wind events were followed by
673 decreases in ^{234}Th deficits in the upper 300 m (Table 3). Decreases in ^{234}Th deficits
674 accompanying wind events may arise from a deepening of the mixed layer, such that deeper
675 water with ^{234}Th closer to equilibrium with ^{238}U is entrained. This phenomenon was noticed by

676 Buesseler et al. (1992) following a storm event in the North Atlantic. Such wind events also may
677 affect particulate ^{234}Th fluxes (via the "mixed-layer pump" concept of Gardner et al., 1995); for
678 example the high trap ^{234}Th flux in the sample with a collection midpoint of March 15, 2005
679 effectively followed the March 12-13 wind event (Table 2, Fig. 14).

680 Schmidt et al. (2002) also noted significant variability in ^{234}Th deficits at the DYFAMED
681 site in May, 1995, although their sampling was confined to the upper 80 m of the water column.
682 They argued that this period represented the transition from a mesotrophic to an oligotrophic
683 system following the spring bloom (Vidussi et al., 2000). Thus advective influences may have
684 significant effects on water column ^{234}Th profiles in the northwestern Mediterranean, especially
685 during the transition from high to low fluxes following the bloom. In such situations, high
686 resolution sampling of water column ^{234}Th profiles is likely to produce considerable variability
687 in ^{234}Th deficits and sediment traps may provide more accurate measures of local settling ^{234}Th
688 flux.

689 An additional contribution to non-steady-state fluxes of ^{234}Th in the northwestern
690 Mediterranean may arise from the periodic inputs of dust from the Sahara Desert. Dust events
691 were observed during the trap deployments in both 2003 (April 29 and May 7) and 2005 (March
692 11 and 26); they were more intense in 2005 than in 2003 (Lee et al., this volume). These events
693 were followed by enhanced mass (Lee et al., this volume) and ^{234}Th fluxes (Table 2). Lee et al.
694 (this volume) concluded that dust served as a catalyst for particle aggregation and sinking. In
695 such cases, water column ^{234}Th deficits also should increase following a dust event, as particulate
696 ^{234}Th is removed from the water column. We do not have sufficient temporal resolution in the
697 water column ^{234}Th data to test this possibility, but it may explain the high deficit observed on
698 March 11, 2005.

5. Summary and Conclusions

We have compared trap ^{234}Th fluxes and water column ^{234}Th profiles in the northwestern Mediterranean in an attempt to reconcile these two indicators of the flux of ^{234}Th. Detailed sediment trap time-series ^{234}Th fluxes at shallow depths (<300 m), above which ^{234}Th deficits were sampled in the water column, provided the opportunity to place water column ^{234}Th profiles taken weeks apart into a context provided by detailed time-series records of local ^{234}Th fluxes. Comparison of the pattern of trap and water column ^{234}Th fluxes at a coastal site shows reasonable agreement over the ~1 month of sampling during the spring bloom in 1999; in contrast, a lack of agreement between the two indicators of flux is evident at the deep-water DYFAMED site over several months of sampling in 2003 and 2005. Rapid changes in water column ^{234}Th profiles over a few days in the spring of both 2003 and 2005 suggest that lateral and vertical advective effects can introduce high-frequency variability into profiles and the resultant estimated deficits of ^{234}Th. Advection can lead to decoupling of water column and trap measures of ^{234}Th flux because the water column deficit is dominated by the "dissolved" ^{234}Th reservoir, while traps collect the settling flux of particulate ^{234}Th. Most of the particulate ^{234}Th (and mass) flux at the DYFAMED site is carried by particles settling faster that 200 m d^{-1} (Lee et al., this volume; Armstrong et al., this volume; Xue and Armstrong, this volume; Szlosek et al., this volume); thus, for a given advective flow field (currents of ~5 – 20 cm s^{-1}), sediment traps are integrating settling fluxes of particulate ^{234}Th over length scales that are ~40 times less than the spatial scale over which water column deficits may be integrated. Wind-induced mixing of the upper water column also can cause short-term variation in the ^{234}Th deficit.

721 Dust events also may contribute to non-steady state variation in ^{234}Th fluxes. If such
722 events catalyze the aggregation and sinking of particles, both water column deficits and trap
723 fluxes may increase together. Even in such cases, however, unless the dust scavenges significant
724 additional dissolved ^{234}Th from the water column, the effect is likely to be greater on particulate
725 ^{234}Th fluxes measured by traps than on those estimated from water column deficits. Our results
726 suggest that sediment trap and water column estimates of ^{234}Th flux provide complementary
727 views of the removal of ^{234}Th from the water column. The two approaches are especially useful
728 in understanding non-steady-state variation in ^{234}Th fluxes in regions such as the northwestern
729 Mediterranean Sea that experience an annual transition from mesotrophic to oligotrophic
730 conditions. In such areas, ^{234}Th fluxes derived from water column profiles may not be reliable
731 indicators of the local flux of ^{234}Th.

732 **Acknowledgements**

733 Sampling at the coastal site in 1999 was supported by the International Atomic Energy
734 Agency (IAEA) and its Marine Environment Laboratories (MEL). Financial support from the US
735 Dept. of Energy, IAEA and Stony Brook University to JKC during a sabbatical leave is
736 gratefully acknowledged. Research at the DYFAMED site during the MedFlux program in 2003
737 and 2005 was supported by the US National Science Foundation and the IAEA. The IAEA is
738 grateful for the support provided to its Marine Environment Laboratories by the Government of
739 the Principality of Monaco. We thank the captains and crews of the *RVs Seward Johnson,*
740 *Endeavor* and *Tethys* for their assistance. We are also grateful for the assistance provided by our
741 MedFlux colleagues M. Peterson, Z. Liu, L. Abramson, and T. Toubal, and for discussions with
742 C. Lee and S. Wakeham. Wind data at the DYFAMED site in 2005 were from the Meteo-France
743 buoy and were provided courtesy of L. Coppola (Observatoire Oceanologique, Villefranche-sur-

744 Mer). Helpful comments were provided by S. B. Moran, K. Buesseler and two anonymous
745 reviewers. This is MedFlux Contribution No. 18 and MSRC Contribution No. 1357.

746 **References**

747 Amiel, D., J. K. Cochran, J. K., Hirschberg, D. J. 2002. Th-234/U-238 disequilibrium as an
748 indicator of the seasonal export flux of particulate organic carbon in the North Water.
749 Deep-Sea Research II 49, 5191-5209.

750 Armstrong, R. A., Lee, C., Peterson, M. L. Cochran, J.K., Wakeham, S.G. Sinking velocity
751 spectra and the ballast ratio hypothesis. Deep-Sea Research II, this volume.

752 Baker, E. T., Milburn, H. B., Tennat, D. A., 1988. Field assessment of sediment trap
753 efficiency under varying flow conditions. Journal of Marine Research 46, 573-592.

754 Benitez-Nelson, C., Buesseler, K. O., Karl, D. M.,Andrews, J. 2001. A time-series study of
755 particulate matter export in the North Pacific subtropical gyre based on ^{234}Th:^{238}U
756 disequilibrium. Deep-Sea Research I 48, 2595-2611.

757 Bethoux, J. P., Gentili, B., Tailliez, D., 1998. Warming and freshwater budget changes
758 in the Mediterranean since the 1940s, their possible relation to the greenhouse effect.
759 Geophysical Research Letters 25, 1023-1026.

760 Buesseler, K. O., 1991. Do upper ocean sediment traps provide an accurate record of particle
761 flux? Nature 353, 420-423.

762 Buesseler, K. O., Antia, A. N., Chen, M., Fowler, S. W. , Gardner , W. D., Gustafsson, O.,
763 Harada, K., Michaels, A. F., Rutgers van der Loeff, M., Sarin, M., Steinberg, D. K.,
764 Trull, T. 2007. An assessment of the use of sediment traps for estimating upper ocean
765 particle fluxes. Journal of Marine Research 65, 345-416..

766 Buesseler, K. O., Bacon, M. P., Cochran, J. K., Livingston, H. D., 1992. Carbon and nitrogen
767 export during the JGOFS North Atlantic Bloom Experiment estimated from Th-234/U-
768 238 disequilibria. Deep-Sea Research I 39, 1115-1137.
769 Buesseler, K. O., Ball, L., Andrews, J., Benitez-Nelson, C., Belastock, R., Chai, F., Chao, Y.,
770 1998. Upper ocean export of particulate organic carbon in the Arabian Sea derived from
771 thorium-234. Deep-Sea Research II 45, 2461-2487.
772 Buesseler, K. O., Ball, L., Andrews, J., Cochran, J. K., Hirschberg, D. J., Bacon, M. P., Fleer, A.,
773 Brzezinski, M., 2001. Upper ocean export of particulate organic carbon and biogenic
774 silica in the Southern Ocean along 170 degrees W. Deep-Sea Research II 48, 4275-4297.
775 Buesseler, K. O., Benitez-Nelson, C. R., Moran, S. B., Burd, A., Charette, M., Cochran, J. K.,
776 Coppola, L., Fisher, N. S., Fowler, S. W., Gardner, W. D., Guo, L. D.,Gustafsson, O.,
777 Lamborg, C., Masqué, P., Miquel, J. C., Passow, U., Santschi, P. H., Savoye, N.,
778 Stewart, G., Trull, T., 2006. An assessment of particulate organic carbon to thorium-
779 234 ratios in the ocean and their impact on the application of ^{234}Th as a POC flux
780 proxy. Marine Chemistry 100, 190-212.
781 Buesseler, K. O., Steinberg, D. K., Michaels, A. F., Johnson, R. J., Andrews, J. E., Valdes, J. R.,
782 Price, J. F. 2000. A comparison of the quantity and quality of material caught in a
783 neutrally buoyant versus surface-tethered sediment trap. Deep-Sea Research I 47, 277-
784 294.
785 Cai, P., Dai, M., Lu, D., Chen, W. (2006) How accurate are ^{234}Th measurements in seawater
786 based on MnO_2-impregnated cartridge technique? Geochemistry Geophysics
787 Geosystems 7, Q03020, doi:10.1029/2005GC001104.

788 Chen, J. H., Edwards, R. L., Wasserburg, G. J., 1986. ^{238}U, ^{234}U and ^{232}Th in seawater. Earth and
789 Planetary Science Letters 80, 241-251.
790 Cochran, J. K., Barnes, C., Achman, D., Hirschberg, D. J., 1995. Thorium-234/Uranium-238
791 disequilibrium as an indicator of scavenging rates and particulate organic carbon fluxes
792 in the Northeast Water Polynya, Greenland. Journal of Geophysical Research 100:
793 4399-4410.
794 Cochran, J. K., Buesseler, K. O., Bacon, M. P., Wang, H., Hirschberg, D. J., Ball, L. Andrews,
795 L., Crossin, G., Fleer, A., 2000. Short-lived thorium isotopes (^{234}Th, ^{228}Th) as
796 indicators of POC export and particle cycling in the Ross Sea, Southern Ocean. Deep-
797 Sea Research II 47: 3451-3490.
798 Cochran, J. K., Masqué, P., 2003. Short-lived U/Th series radionuclides in the ocean: Tracers for
799 scavenging rates, export fluxes and particle dynamics, In: Uranium-Series
800 Geochemistry (B. Bourdon, G. M. Henderson, C. C. Lundstrom, S. P. Turner, eds)
801 Reviews in Mineralogy & Geochemistry 52, pp. 461-492.
802 Conan, P., Millot, C., 1995. Variability of the Northern Current off Marseilles, western
803 Mediterranean Sea, from February to June 1992. Oceanologica Acta 18, 193–205.
804 Edwards, A. W. F., 1992. *Likelihood*. Johns Hopkins University Press, Baltimore, MD, USA.
805 Fieux, M., 1994. Formation d'eau dense sur le plateau continental du Golfe du Lion, Colloque
806 International du CNRS sur: La Formation des Eaux Oceaniques Profondes., 215, 165-
807 189.
808 Gardner, W. D., 1980. Sediment trap dynamics and calibration: a laboratory evaluation. Journal
809 of Marine Research 38: 17-39.
810 Gardner, W. D., Chung, S. P, Richardson, M. J., Walsh, I. D. 1995. The oceanic mixed-layer
811 pump. Deep-Sea Research II 42, 757-775.

812 Gust, G., Bowles, W., Giordano, S., Huttel, M., 1996. Particle accumulation in a cylindrical
813 sediment trap under laminar and turbulent steady flow: An experimental approach.
814 Aquatic Sciences 58, 297-326.
815 Gust, G., Kozerski, H.-P., 2000. In situ sinking particle flux from collection rates of cylindrical
816 traps. Marine Ecology Progress Series 208, 93-106.
817 Gustafsson, O., Andersson, P., Kukulska, Z., Broman, D., Hajdu, S., Ingri, J., 2004. Evaluation
818 of collection efficiency of upper ocean sub-photic layer sediment traps: a 24-month in
819 situ calibration in the open Baltic Sea using ^{234}Th. Limnology and Oceanography:
820 Methods 2, 62-74.
821 Hilborn, R., Mangel, M., 1997. The Ecological Detective: Confronting Models with Data.
822 Princeton University Press, Princeton, NJ, USA.
823 Hung, C.-C., Moran, S. B., Cochran, J. K., Guo, L., Santschi, P. H. 2008. Comment on ‘‘How
824 accurate are ^{234}Th measurements in seawater based on the MnO_2-impregnated cartridge
825 technique?’’ by Pinghe Cai et al., Geochemistry Geophysics Geosystems, 9, Q02009,
826 doi:10.1029/2007GC001770.
827 Hurtt, G. C., Armstrong, R. A., 1994. A pelagic ecosystem model calibrated with BATS data.
828 Deep-Sea Res. II 43:653-683.

829 Ku, T.-L., Musakabe, M., 1990. Testing Biological Control of Elemental Removal in Surface
830 Ocean with $^{7}Be/^{10}Be$ and U/Th Series Isotopes. In: Isotopic Tracers in U. S. JGOFS (M.
831 P. Bacon, R.F. Anderson, eds), U.S. JGOFS Planning and Coordination Office, Woods
832 Hole, MA, pp. 101-105.

833 Lee, C., Peterson, M. L., Wakeham, S. G., Armstrong, R. A., Cochran, J. K., Miquel, J. C.,
834 Fowler, S. W., Hirschberg, D., Beck, A., Xue, J., 2008. Particulate organic matter and
835 ballast fluxes measured using Time-Series and Settling Velocity sediment traps in the
836 northwestern Mediterranean Sea**.** Deep-Sea Research II, this volume

837 Livingston, H. D., Cochran, J. K., 1987. Determination of transuranic and thorium isotopes in
838 ocean water - in solution and in filterable particles. Journal of Radioanalytical and
839 Nuclear Chemistry 115: 299-308.

840 Metropolis, N., Rosenbluth, A. W., Rosenbluth, M. N., Teller, A. H., Teller, E., 1953. Equation
841 of state calculations by fast computing machines. Journal of Chemical Physics 21, 1087-
842 1092.

843 Millot, C., 1999. Circulation in the Western Mediterranean Sea.. Journal of Marine
844 Systems 20, 432-442.

845 Miquel J. C., Fowler, S. W., La Rosa , J., Buat-Menard, P., 1994. Dynamics of the downward
846 flux of particles and carbon in the open NW Mediterranean Sea. Deep-Sea Research 41,
847 242-261.

848 Miquel, J. C., La Rosa, J., 1999. Suivi à long term des flux particulaires au site DYFAMED
849 (mer Ligure, Méditerranée occidentale). Océanis 25, 303-318.

850 Moran, S. B., Weinstein, S. E., Edmonds, H. N., Smith, J. N., Kelly, R. P., Pilson, M. E. Q.,
851 Harrison, W. G., 2003. Does $^{234}Th/^{238}U$ disequilibrium provide an accurate record of

852 the export flux of particulate organic carbon from the upper ocean? Limnology and
853 Oceanography 48, 1018-1029.
854 Pates, J. M., Muir, G. K. P., 2007. Uranium-salinity relationships in the Mediterranean:
855 implications for ^{234}Th:^{238}U particle flux studies. Marine Chemistry, 106, 530-545..
856 Peterson, M. L., Thoreson, D. S., Hedges, J. I., Lee, C., Wakeham, S. G., 1993. Field evaluation
857 of a valved sediment trap. Limnology and Oceanography 38, 1741-1761.
858 Peterson, M. L., Wakeham, S. G., Lee, C., Askea, M., Miquel, J. C., 2005. Novel techniques for
859 collection of sinking particles in the ocean and determining their settling rates.
860 Limnology and Oceanography Methods 3, 520-532.
861 Peterson, M. L., Fabres, J., Wakeham, S. G., Lee, C., Miquel, J. C., 2008. Sampling the verrtical
862 particle flux in the upper water column using a large diameter free-drifting NetTrap
863 adapted to an Indented Rotating Sphere sediment trap. Deep-Sea Research II, this
864 volume.
865 Rutgers van der Loeff, M., Moore, W. S., 1999. Determination of natural radioactive tracers. In:
866 Methods of Seawater Analysis, 3d ed. (K. Grasshof, M. Ehrhardt, K. Kremling, eds.)
867 Verlag Chemie, Weinheim, pp. 365-397.
868 Rutgers van der Loeff, M., Sarin, M. M., Baskaran, M., Benitez-Nelson, C., Buesseler, K. O.,
869 Charette, M., Dai, M., Gustafsson, O., Masqué, P., Morris, P. J., Orlandini, K.,
870 Rodriguez y Baena, A., Savoye, N., Schmidt, S., Turnewitsch, R., Voge, I., Waples, J.
871 T., 2006. A review of present techniques and methodological advances in analyzing
872 ^{234}Th in aquatic systems. Marine Chemistry 100, 190-212.

873 Savoye, N., Benitez-Nelson, C., Burd, A. B., Cochran, J. K., Charette, M., Buesseler, K. O.,
874 Jackson, G. A., Roy-Barman, M., Schmidt, S., Elskens, M., 2006. ^{234}Th sorption and
875 export models in the water column: A review. Marine Chemistry 100, 234-249.
876 Schmidt, S., Andersen, V., Belviso, S., Marty, J.-C., 2002. Strong seasonality in particle
877 dynamics of north-western Mediterranean surface waters as revealed by ^{234}Th/^{238}U.
878 Deep-Sea Research I 49, 1507-1518.
879 Siegel, D. A., Deuser, W. G., 1997. Trajectories of sinking particles in the Sargasso Sea:
880 Modeling of statistical funnels above deep-ocean sediment traps. Deep-Sea Research 44:
881 1519-1541.
882 Siegel, D. A., Granata, T. C., Michaels, A. F., Dickey, T. D., 1990. Mesoscale eddy diffusion,
883 particle sinking, and the interpretation of sediment trap data. Journal of Geophysical
884 Research 95: 5305-5311.
885 Speicher, E. A., Moran, S. B., Burd, A. B., Delfanti, R., Kaberi, H., Kelly, R. P., Papucci, C.,
886 Smith, J. N., Stavrakakis, S., Torricelli, L., Zervakis, V., 2006. Particulate organic carbon
887 export fluxes and size-fractionated POC/^{234}Th ratios in the Ligurian, Tyrrhenian and
888 Aegean Seas. Deep-Sea Research I 53, 1810-1830.
889 Stewart, G., Cochran, J. K., Miquel, J. C., Masqué, P., Szlosek, J., Rodriguez y Baena, A. M.,
890 Fowler, S. W., Gasser, B., Hirschberg, D. J., 2007. Comparing POC export from
891 ^{234}Th/^{238}U and ^{210}Po/^{210}Pb disequilibria with estimates from sediment traps in the
892 northwest Mediterranean. Deep-Sea Research I, 54, 1549-1570.
893 Szlosek, J., Cochran, J. K., Miquel, J. C., Masqué, P., Armstrong, R. A., Fowler, S. A., Gasser,
894 B., Hirschberg, D. J., 2008. Particulate organic carbon-^{234}Th relationships in particles

separated by settling velocity in the Northwest Mediterranean. Deep-Sea Research II, this volume.

Vidussi, F., Marty, J.-C., Chiaverini, J., 2000. Phytoplankton pigment variations during te transition from spring bloom to oliogotrophy in the northwestern Mediterranean Sea. Deep-Sea Research I 47, 423-445.

Wakeham, S. G., Lee, C., Peterson, M. L., Liu, Z., Szlosek, J., Putnam, I. F., Xue, J. 2008. Organic biomarkers in the twilight zone- Time series and settling velocity sediment traps during MedFlux. Deep-Sea Research II, accepted.

Wyse, E., Lee, S.-H., Rodriguez y Baena, A., Azemard, S., Miquel, J.-C., Gastaud, J., Pham, M. K., Povinec, P. P., DeMora, S., 2006. Measurement of Radioisotopes in Marine Samples by Sector Field ICP-MS. In: Isotopes in Environmental Studies, IAEA-CSP-26, IAEA, Vienna, pp. 499-500.

Xue, J., Armstrong, R. A., 2008. A new method for estimating settling velocities of sinking particles in the open ocean. Deep-Sea Research II, this volume.

Table 1: Water column ^{234}Th data- Northwest Mediterranean Sea

Sampling Date (mm/dd/yyyy)	Day of Year	Depth (m)	Particulate ^{234}Th (> 1 μm) (dpm/L)	Dissolved ^{234}Th (dpm/L)	Total ^{234}Th (dpm/L)
Coastal site (1999)					
03/10-12/1999	69-71	2	0.455 ± 0.024	1.49 ± 0.07	1.95 ± 0.07
		25	0.387 ± 0.017	1.88 ± 0.20	2.27 ± 0.20
		40	0.346 ± 0.018	1.30 ± 0.07	1.64 ± 0.07
		65	0.366 ± 0.016	1.57 ± 0.29	1.94 ± 0.29
		90	0.321 ± 0.015	1.78 ± 0.24	2.10 ± 0.24
03/16-19/1999	75-78	2	0.376 ± 0.024	1.77 ± 0.09	2.15 ± 0.09
		25	-	-	1.38 ± 0.03
		40	-	-	1.18 ± 0.08
		65	0.367 ± 0.012	0.98 ± 0.07	1.35 ± 0.07
		90	0.285 ± 0.009	1.45 ± 0.21	1.74 ± 0.21
03/24/1999	83	5	0.107 ± 0.015	1.46 ± 0.47	1.57 ± 0.47
		25	0.213 ± 0.025	1.43 ± 0.11	1.64 ± 0.11
		40	0.091 ± 0.007	1.76 ± 0.21	1.85 ± 0.21
		65	0.208 ± 0.011	1.57 ± 0.11	1.78 ± 0.11
		90	0.307 ± 0.029	1.79 ± 0.11	2.10 ± 0.11
03/31/1999	88	5	0.065 ± 0.010	1.10 ± 0.19	1.16 ± 0.19
		25	0.079 ± 0.012	1.15 ± 0.10	1.23 ± 0.10
		40	0.120 ± 0.007	1.43 ± 0.10	1.55 ± 0.10
		65	0.259 ± 0.032	1.37 ± 0.25	1.63 ± 0.25
		90	0.171 ± 0.010	1.42 ± 0.09	1.60 ± 0.09
04/07/1999	95	120	0.054 ± 0.004	1.72 ± 0.14	1.78 ± 0.14
		150	0.234 ± 0.011	1.65 ± 0.04	1.88 ± 0.05
		200	0.267 ± 0.012	1.69 ± 0.14	1.95 ± 0.14
DYFAMED Site (2003)					
03/04/2003	63	2	0.221 ± 0.004	2.13 ± 0.14	2.35 ± 0.14
		20	0.179 ± 0.002	2.09 ± 0.16	2.28 ± 0.16
		50	0.259 ± 0.004	2.28 ± 0.14	2.55 ± 0.14
		75	0.212 ± 0.003	2.36 ± 0.21	2.58 ± 0.21
		100	0.238 ± 0.004	2.44 ± 0.17	2.68 ± 0.17
		150	0.147 ± 0.004	2.46 ± 0.18	2.61 ± 0.18
		200	0.150 ± 0.002	2.63 ± 0.16	2.78 ± 0.16

Table 1 (cont): Water column ^{234}Th data- Northwest Mediterranean Sea

Sampling Date (mm/dd/yyyy)	Day of Year	Depth (m)	Particulate ^{234}Th (> 1 μm) (dpm/L)	Dissolved ^{234}Th (dpm/L)	Total ^{234}Th (dpm/L)
05/07/2003	127	2	0.244 ± 0.007	2.61 ± 0.25	2.85 ± 0.25
		20	0.138 ± 0.004	2.35 ± 0.16	2.49 ± 0.16
		40	0.281 ± 0.008	1.88 ± 0.15	2.16 ± 0.15
		60	0.153 ± 0.002	2.33 ± 0.18	2.49 ± 0.18
		100	0.104 ± 0.140	2.19 ± 0.16	2.29 ± 0.21
		150	0.223 ± 0.039	2.21 ± 0.12	2.44 ± 0.12
		200	0.235 ± 0.056	2.25 ± 0.14	2.48 ± 0.15
05/11/2003	131	20	0.160 ± 0.008	2.05 ± 0.18	2.21 ± 0.18
		45	0.388 ± 0.009	2.09 ± 0.21	2.48 ± 0.21
		75	0.182 ± 0.002	2.44 ± 0.19	2.63 ± 0190
		100	0.231 ± 0.006	2.10 ± 0.16	2.33 ± 0.16
		150	0.242 ± 0.005	2.45 ± 0.14	2.70 ± 0.14
		200	0.188 ± 0.005	2.45 ± 0.14	2.64 ± 0.14
05/13/2003	133	2	0.175 ± 0.004	3.22 ± 0.25	3.39 ± 0.25
		20	0.125 ± 0.005	1.72 ± 0.45	1.85 ± 0.45
		50	0.191 ± 0.003	2.38 ± 0.26	2.57 ± 0.26
		60	0.157 ± 0.004	2.61 ± 0.24	2.77 ± 0.24
		100	0.084 ± 0.003	2.30 ± 0.12	2.38 ± 0.12
		150	0.095 ± 0.003	1.72 ± 0.12	1.82 ± 0.12
		200	0.201 ± 0.005	3.70 ± 0.20	3.90 ± 0.20
06/30/2003	181	20	0.309 ± 0.008	1.79 ± 0.12	2.10 ± 0.12
		50	0.676 ± 0.014	1.19 ± 0.10	1.86 ± 0.10
		75	0.169 ± 0.004	2.38 ± 0.20	2.55 ± 0.20
		100	0.147 ± 0.009	2.67 ± 0.09	2.82 ± 0.09
		150	0.200 ± 0.012	2.32 ± 0.09	2.52 ± 0.09
		200	0.236 ± 0.016	2.46 ± 0.09	2.70 ± 0.09

Table 1 (cont): Water column ^{234}Th data- Northwest Mediterranean Sea

Sampling Date (mm/dd/yyyy)	Day of Year	Depth (m)	Particulate ^{234}Th (> 1 μm) (dpm/L)	Dissolved ^{234}Th (dpm/L)	Total ^{234}Th (dpm/L)
DYFAMED Site (2005)					
03/02/2005	61	5	-	-	2.69 ± 0.16
(Niskin)		30	-	-	2.34 ± 0.15
		70	-	-	2.33 ± 0.15
		110	-	-	2.38 ± 0.16
		150	-	-	2.80 ± 0.19
		200	-	-	2.59 ± 0.14
		300	-	-	3.09 ± 0.31
		400	-	-	2.75 ± 0.19
		450	-	-	2.62 ± 0.17
		500	-	-	2.36 ± 0.15
		700	-	-	2.64 ± 0.16
		1000	-	-	2.59 ± 0.17
03/08-09/2005	67-68	5	-	-	2.34 ± 0.13
(Niskin)		25	-	-	2.28 ± 0.13
		60	-	-	2.15 ± 0.12
		100	-	-	2.25 ± 0.12
		100	-	-	2.34 ± 0.14
		125	-	-	2.33 ± 0.15
		150	-	-	2.16 ± 0.12
		200	-	-	2.51 ± 0.14
		200	-	-	2.64 ± 0.14
		250	-	-	2.50 ± 0.12
		300	-	-	2.83 ± 0.14
		350	-	-	2.65 ± 0.16
		500	-	-	2.59 ± 0.14
		750	-	-	2.79 ± 0.16
		900	-	-	2.62 ± 0.15
		1050	-	-	2.74 ± 0.16
		1500	-	-	2.87 ± 0.16
		2000	-	-	2.88 ± 0.18
		2000	-	-	2.89 ± 0.17
		2000	-	-	2.77 ± 0.15
		2000	-	-	2.66 ± 0.16
		2000	-	-	2.58 ± 0.14

Table 1 (cont): Water column ^{234}Th data- Northwest Mediterranean Sea

Sampling Date (mm/dd/yyyy)	Day of Year	Depth (m)	Particulate ^{234}Th (> 1 μm) (dpm/L)	Dissolved ^{234}Th (dpm/L)	Total ^{234}Th (dpm/L)
03/09/2005	68	25	0.382 ± 0.015	1.74 ± 0.05	2.12 ± 0.05
(Pump)		60	0.419 ± 0.018	1.76 ± 0.05	2.18 ± 0.05
		100	0.379 ± 0.017	2.28 ± 0.12	2.66. ± 0.12
		150	0.398 ± 0.017	1.81 ± 0.06	2.21 ± 0.06
		300	0.203 ± 0.001	2.77 ± 0.11	2.97 ± 0.11
		400	0.157 ± 0.003	2.63 ± 0.10	2.79 ± 0.10
		600	0.150 ± 0.034	2.37 ± 0.11	2.52 ± 0.11
		1500	0.120 ± 0.020	2.67 ± 0.12	2.79 ± 0.12
		1800	0.118 ± 0.022	2.52 ± 0.12	2.64 ± 0.12
03/11/2005	70	5	-	-	2.05 ± 0.15
(Niskin)		25	-	-	1.87 ± 0.13
		50	-	-	1.73 ± 0.12
		75	-	-	1.79 ± 0.13
		100	-	-	1.55 ± 0.12
		125	-	-	1.86 ± 0.14
		150	-	-	2.41 ± 0.17
		200	-	-	2.37 ± 0.17
		275	-	-	2.50 ± 0.18
		350	-	-	2.66 ± 0.17
		500	-	-	2.58 ± 0.18
		1000	-	-	2.69 ± 0.17
03/13/2005	72	5	0.286 ± 0.022	2.13 ± 0.08	2.42 ± 0.08
(Pump)		25	0.504 ± 0.030	1.92 ± 0.05	2.42 ± 0.06
		75	0.229 ± 0.023	2.46 ± 0.07	2.68 ± 0.07
		100	0.244 ± 0.004	2.23 ± 0.07	2.47 ± 0.07
		200	0.178 ± 0.002	2.58 ± 0.10	2.76 ± 0.10
		400	0.175 ± 0.004	2.47 ± 0.14	2.65 ± 0.14
		500	0.212 ± 0.026	2.20 ± 0.08	2.41 ± 0.08
		800	0.167 ± 0.028	2.37 ± 0.07	2.54 ± 0.08
		900	0.127 ± 0.029	2.28 ± 0.06	2.41 ± 0.07

Table 1 (cont): Water column ^{234}Th data- Northwest Mediterranean Sea

Sampling Date (mm/dd/yyyy)	Day of Year	Depth (m)	Particulate ^{234}Th (> 1 μm) (dpm/L)	Dissolved ^{234}Th (dpm/L)	Total ^{234}Th (dpm/L)
03/14/2005	73	5	-	-	2.29 ± 0.12
(Niskin)		25	-	-	2.49 ± 0.13
		50	-	-	2.60 ± 0.14
		75	-	-	2.40 ± 0.13
		100	-	-	2.18 ± 0.13
		100	-	-	2.44 ± 0.14
		125	-	-	2.31 ± 0.11
		150	-	-	2.59 ± 0.14
		175	-	-	2.55 ± 0.14
		200	-	-	2.61 ± 0.15
		250	-	-	2.78 ± 0.16
		300	-	-	2.72 ± 0.17
		750	-	-	2.67 ± 0.17
		1000	-	-	2.36 ± 0.13
04/29-30/2005	119-120	5	-	-	2.39 ± 0.15
(Niskin)		15	-	-	2.72 ± 0.16
		25	-	-	2.50 ± 0.16
		35	-	-	2.33 ± 0.15
		50	-	-	2.38 ± 0.12
		50	-	-	2.67 ± 0.14
		60	-	-	2.76 ± 0.15
		75	-	-	2.79 ± 0.16
		90	-	-	2.57 ± 0.14
		100	-	-	2.49 ± 0.15
		125	-	-	2.63 ± 0.16
		150	-	-	2.98 ± 0.17
		175	-	-	2.80 ± 0.16
		200	-	-	3.09 ± 0.17
		300	-	-	3.17 ± 0.20
		500	-	-	2.72 ± 0.15
		500	-	-	2.73 ± 0.15
		750	-	-	2.71 ± 0.15

Table 2: Sediment trap ^{234}Th fluxes

Midpoint of Sample Collection (mm/dd/yyyy)	Day of Year	^{234}Th Flux (dpm m^{-2} d^{-1})	^{234}Th Flux (dpm m^{-2} d^{-1})	^{234}Th Flux (dpm m^{-2} d^{-1})	Mean ^{234}Th Flux (dpm m^{-2} d^{-1})
Coastal Site (170 m)					
Trap type		PPS-3	PPS-4	PPS-5	
03/11/1999	70	3466	2076	3758	3100 ± 898
03/13/1999	72	1597	1613	1937	1715 ± 192
03/15/1999	74	2969	3052	3022	3014 ± 42
03/17/1999	76	1864	2419	3203	2495 ± 673
03/19/1999	78	3448	2592	4275	3438 ± 841
03/21/1999	80	2081	2468	3571	2707 ± 773
03/23/1999	82	2587	4644	3804	3678 ± 1034
03/25/1999	84	4128	1583	2521	2744 ± 1287
03/27/1999	86	4297	3581	4126	4001 ± 364
03/29/1999	88	4320	3633	3513	3822 ± 435
03/31/1999	90	1005	1690	1738	1478 ± 410
04/02/1999	92	941	333	431	568 ± 326
DYFAMED Site (238 m)					
03/08/2003	67	2288 ± 194			
03/13/2003	72	1715 ± 155			
03/18/2003	77	2279 ± 145			
03/23/2003	82	1153 ± 104			
03/28/2003	87	596 ± 66			
04/03/2003	92	301 ± 28			
04/09/2003	98	317 ± 25			
04/15/2003	104	486 ± 25			
04/21/2003	110	516 ± 22			
04/27/2003	116	307 ± 16			
05/03/2003	122	502 ± 17			
DYFAMED Site (117 m)					
05/16/2003	135	544 ± 29			
05/20/2003	139	417 ± 26			
05/24/2003	143	307 ± 22			
05/28/2003	147	232 ± 18			
06/01/2003	151	-			
06/05/2003	155	59 ± 12			
06/09/2003	159	32 ± 10			
06/13/2003	163	51 ± 10			
06/17/2003	167	-			
06/22/2003	172	17 ± 7			
06/27/2003	177	12 ± 5			

Table 2 (cont.) : Sediment trap ^{234}Th fluxes

Midpoint of Sample Collection (mm/dd/yyyy)	Day of Year	^{234}Th Flux (dpm m^{-2} d^{-1})
DYFAMED Site (313 m)		
03/06/2005	65	2505 ± 77
03/11/2005	70	2261 ± 64
03/16/2005	75	875 ± 42
03/21/2005	80	1485 ± 47
03/26/2005	85	1320 ± 41
03/31/2005	90	2494 ± 46
04/05/2005	95	900 ± 25
04/10/2005	100	239 ± 13
04/15/2005	105	469 ± 16
04/20/2005	110	294 ± 12
04/25/2005	115	73 ± 6

Table 3: Water column ^{234}Th deficits (10^4 dpm m^{-2})

Coastal Site							
Sampling date (mm/dd/yyyy)	03/11/1999	03/18/1999	03/24/1999	03/31/1999			
Day of Year	70	77	83	90			
0-90 m	6.1 ± 1.0	10.5 ± 0.4	7.8 ± 0.8	10.8 ± 0.8			
DYFAMED Site							
Sampling date (mm/dd/yyyy)	03/04/2003	05/07/2003	05/11/2003	05/13/2003	06/30/2003		
Day of Year	63	127	131	133	181		
0-100 m	2.1 ± 0.8	2.8 ± 0.9	2.9 ± 0.9	2.0 ± 1.4	4.6 ± 0.7		
0-200 m	2.5 ± 1.4	5.6 ± 1.3	3.9 ± 1.3	4.2 ± 1.7	5.2 ± 0.9		
Sampling date (mm/dd/yyyy)	03/02/2005	03/08-09/2005	03/09/2005	03/11/05	03/13/2005	03/14/2005	04/29-30/2005
Day of Year	61	67-68	68	70	72	73	119-120
0-300 m	2.4 ± 2.9*	9.3 ± 1.4	7.5 ± 1.2*	14.1 ± 1.7	2.2 ± 1.3*	4.6 ± 1.4*	-4.1 ± 17*

*Deficits calculated from Th measured in small volume (Niskin) samples; all others from in situ pumps

Figures

Fig. 1: Map showing location of coastal (open square) and DYFAMED (filled square) sampling sites.

Fig. 2: Hydrographic data for coastal site during times of water column ^{234}Th sampling.

Fig. 3: ^{234}Th water column profiles at coastal site- 1999. Dashed line is ^{238}U activity. Open symbols are particulate (>1 μm) ^{234}Th; solid symbols are total ^{234}Th obtained by summing particulate + dissolved (not shown) activities.

Fig. 4: Hydrographic data at DYFAMED site- March, 2005: a) salinity, b) fluorescence.

Fig. 5: ^{234}Th water column profiles at DYFAMED site- 2003. Dashed line is ^{238}U activity. Open symbols are particulate (>1 μm) ^{234}Th; solid symbols are total ^{234}Th obtained by summing particulate + dissolved (not shown) activities.

Fig. 6: ^{234}Th water column profiles at DYFAMED site- 2005. Dashed line is ^{238}U activity. Open symbols are particulate (>1 μm) ^{234}Th; solid symbols are total ^{234}Th obtained by summing particulate + dissolved (not shown) activities. When no particulate activity is shown, only total ^{234}Th was measured.

Fig. 7: Water column ^{234}Th deficits vs. time at coastal site. Open circles + dashed line represent the deficits predicted from the sediment trap fluxes at 170 m (Eq. 6) with $\alpha = 1$. Individual points (marked with "x") are measured deficits (0-90 m) from ^{234}Th water column profiles (Fig. 5; Table 3).

Fig. 8: ^{234}Th flux vs. time at coastal site. Solid lines represent histogram of measured trap flux at 170 m. "x" denotes steady-state ^{234}Th fluxes calculated from measured ^{234}Th water column deficits to 90 m (Eq. 2). Dashed lines are non-steady state ^{234}Th fluxes determined from two successive water column ^{234}Th profiles (Eq. 7)

Fig. 9: Water column ^{234}Th deficit vs. time at DYFAMED site- 2003. Open circles + dashed line represent the deficits predicted from the sediment trap fluxes at 238 m (day of year 65-126) and at 117 m (day of year 134 – 178; Eq. 6) for a scaling factor, $\alpha = 1$. Open squares + dashed line are predicted deficits, with $\alpha = 2.1$ (effectively corresponding to a trapping efficiency of ~50%). Individual points marked with "x" are deficits (0-200 m) obtained from water column ^{234}Th profiles (Fig. 7); solid square at day-of-year 181 is the deficit integrated to 100 m. Offset in the model-derived deficit curves at day of year 134 corresponds to the fact that the trap fluxes were measured at 238 m during the first deployment and at 117 m during the second and was produced by scaling the curves for the offset between the water column deficit measured in 0-100 m relative to that in 0-200 m in May when the trap turnaround occurred.

Fig. 10: ^{234}Th flux vs. time at DYFAMED site- 2003. Solid lines represent histogram of measured trap fluxes at 238 m (day of year 65 – 126) and 117 m (day of year 134 - 178). "x" denotes steady-state ^{234}Th fluxes calculated from measured ^{234}Th water column deficits to 200 m (Eq. 2). Dashed lines are non-steady state ^{234}Th fluxes determined from two successive water column ^{234}Th profiles (Eq. 7). An average of the deficits of casts 2-4 (shown as "*" at day of year ~130) was used as the effective second time point in this calculation.

Fig. 11: Water column ^{234}Th deficit vs. time at DYFAMED site- 2005. Open circles + dashed line represent the deficits predicted from the sediment trap fluxes at 313 m (day of year 63 - 117; Eq. 6). Individual points (marked with "x") are measured deficits (0-300 m) from water column ^{234}Th profiles (Fig. 8)

Fig. 12: ^{234}Th flux vs. time at DYFAMED site- 2005. Solid lines represent histogram of measured trap flux at 313 m (day of year 63 – 117). "x" denotes steady-state ^{234}Th fluxes calculated from measured ^{234}Th water column deficits to 300 m (Eq. 2). Dashed lines are non-steady state ^{234}Th fluxes determined from two successive water column ^{234}Th profiles (Eq. 7). An average of the deficits of casts 2-6 (shown as "*" at day of year ~70) was used as the effective second time point in this calculation.

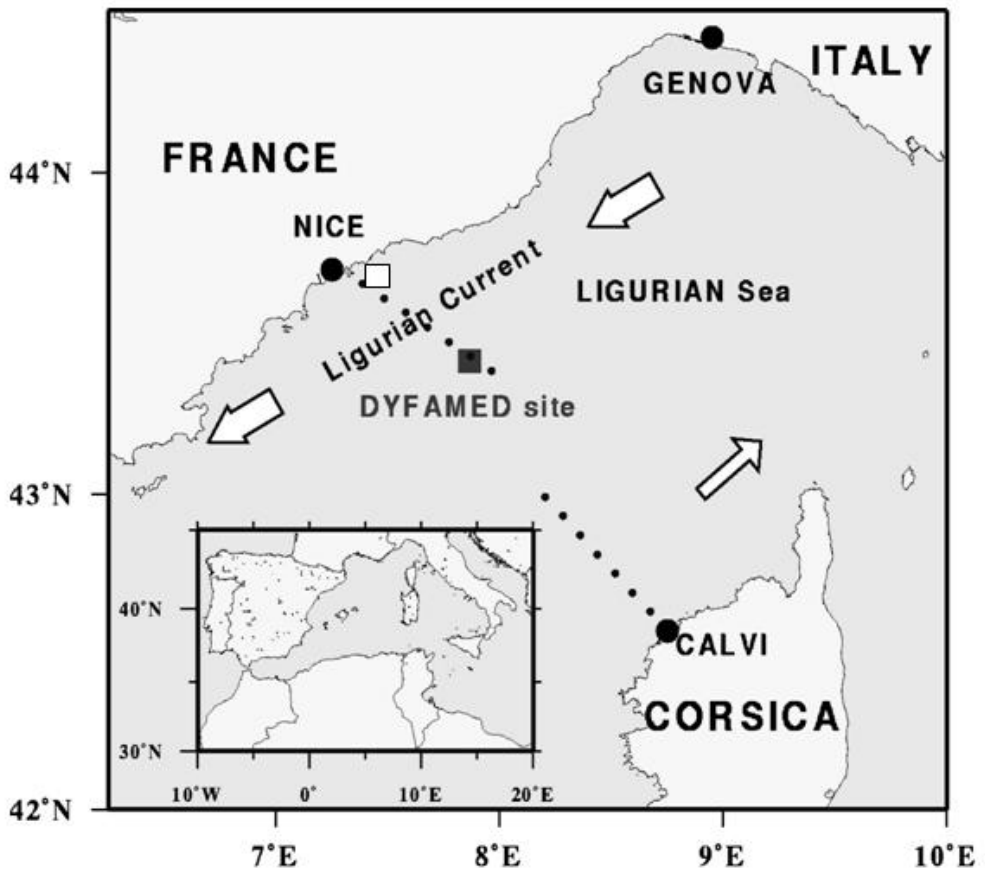
ITALY
GENOVA
FRANCE
44°N
NICE
Ligurian Current
LIGURIAN Sea
DYFAMED site
43°N
40°N
30°N
10°W
0°
10°E
20°E
CALVI
CORSICA
42°N
7°E
8°E
9°E
10°E

Figure 1

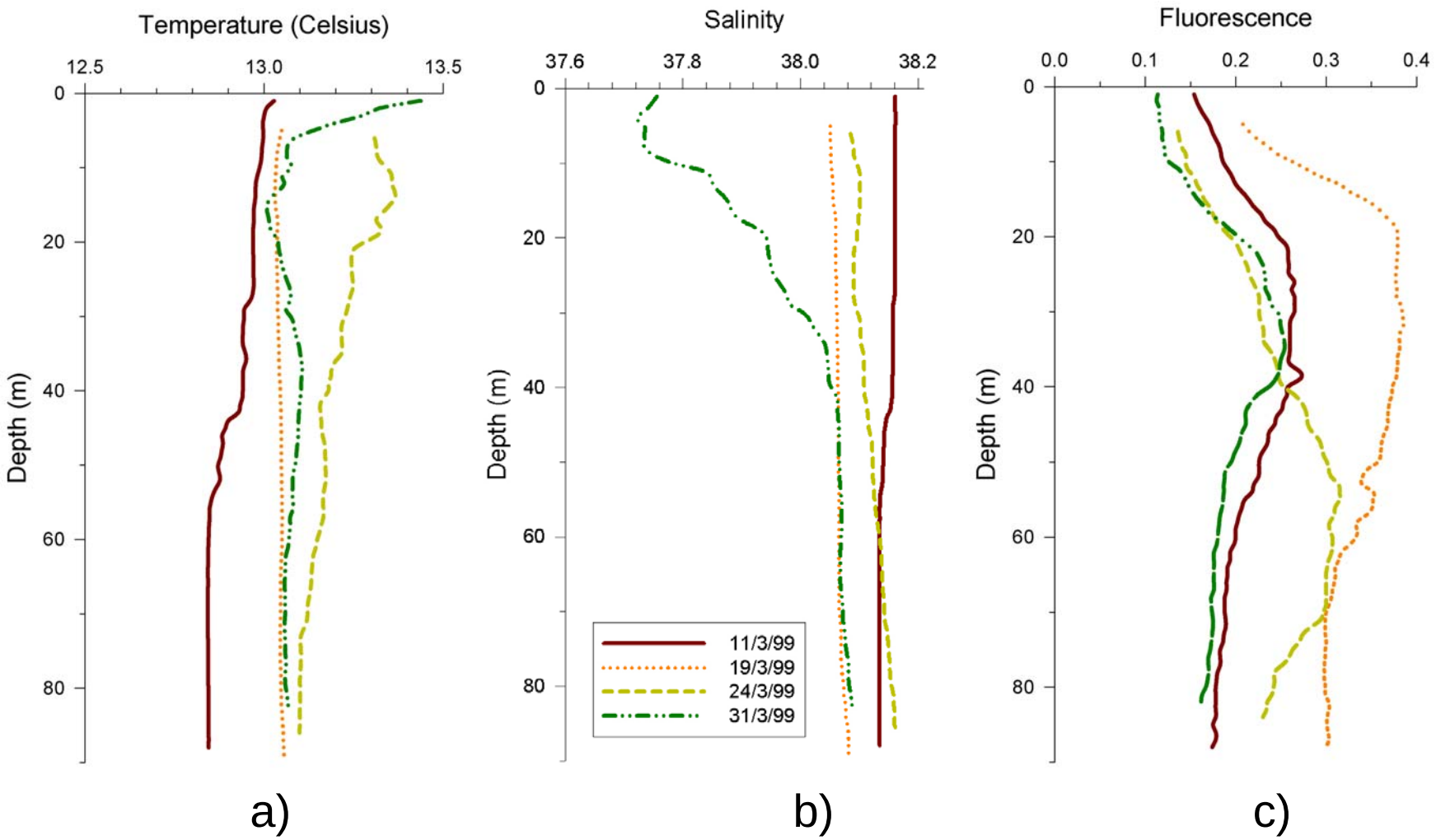
Temperature (Celsius)
12.5
13.0
13.5
Depth (m)
0
20
40
60
80
a)
Salinity
37.6
37.8
38.0
38.2
Depth (m)
0
20
40
60
80
11/3/99
19/3/99
24/3/99
31/3/99
b)
Fluorescence
0.0
0.1
0.2
0.3
0.4
Depth (m)
0
20
40
60
80
c)

Figure 2

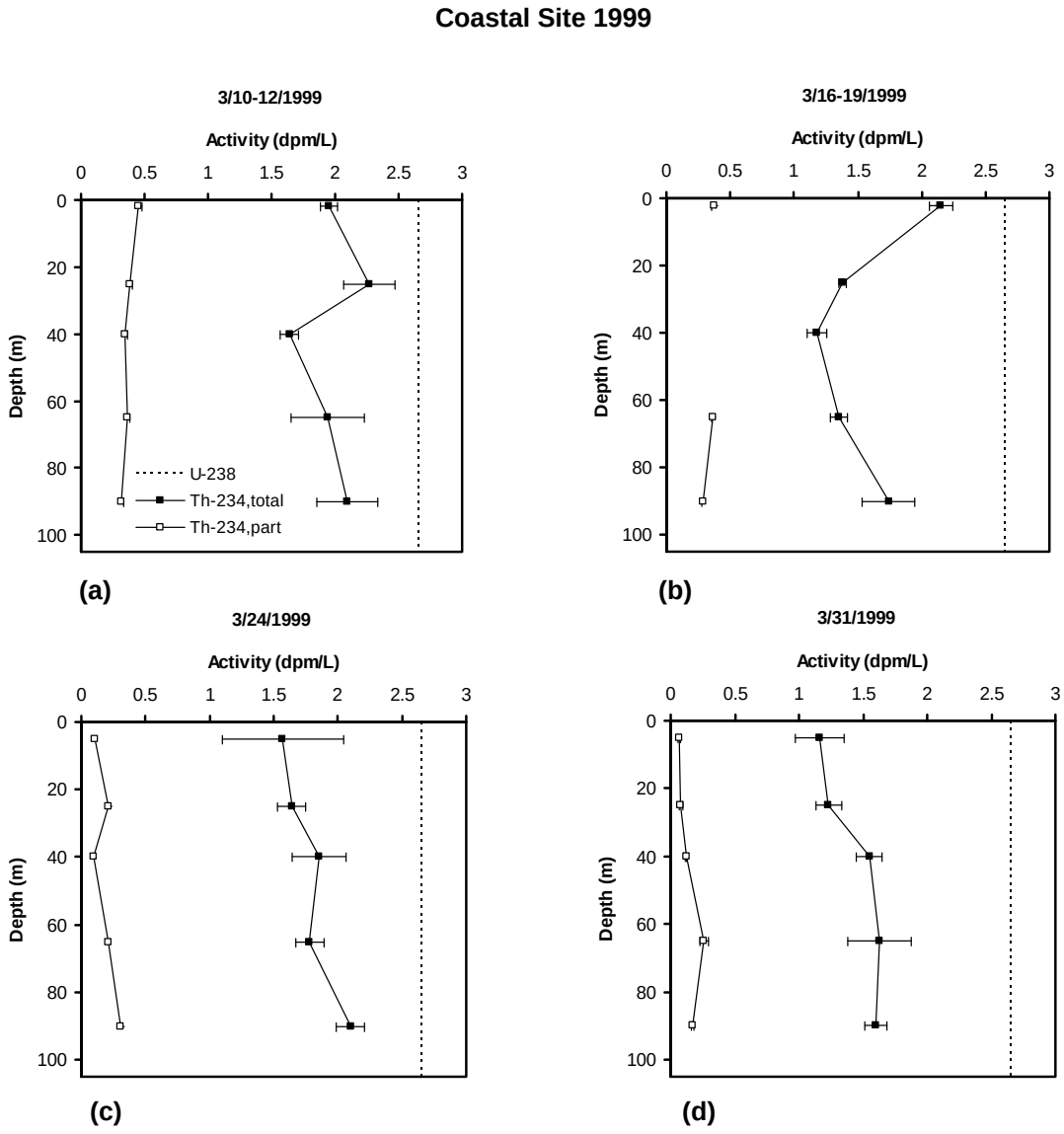
Coastal Site 1999
3/10-12/1999
Activity (dpm/L)
Depth (m)
U-238
Th-234,total
Th-234,part
(a)
3/16-19/1999
(b)
3/24/1999
(c)
3/31/1999
(d)

Figure 3

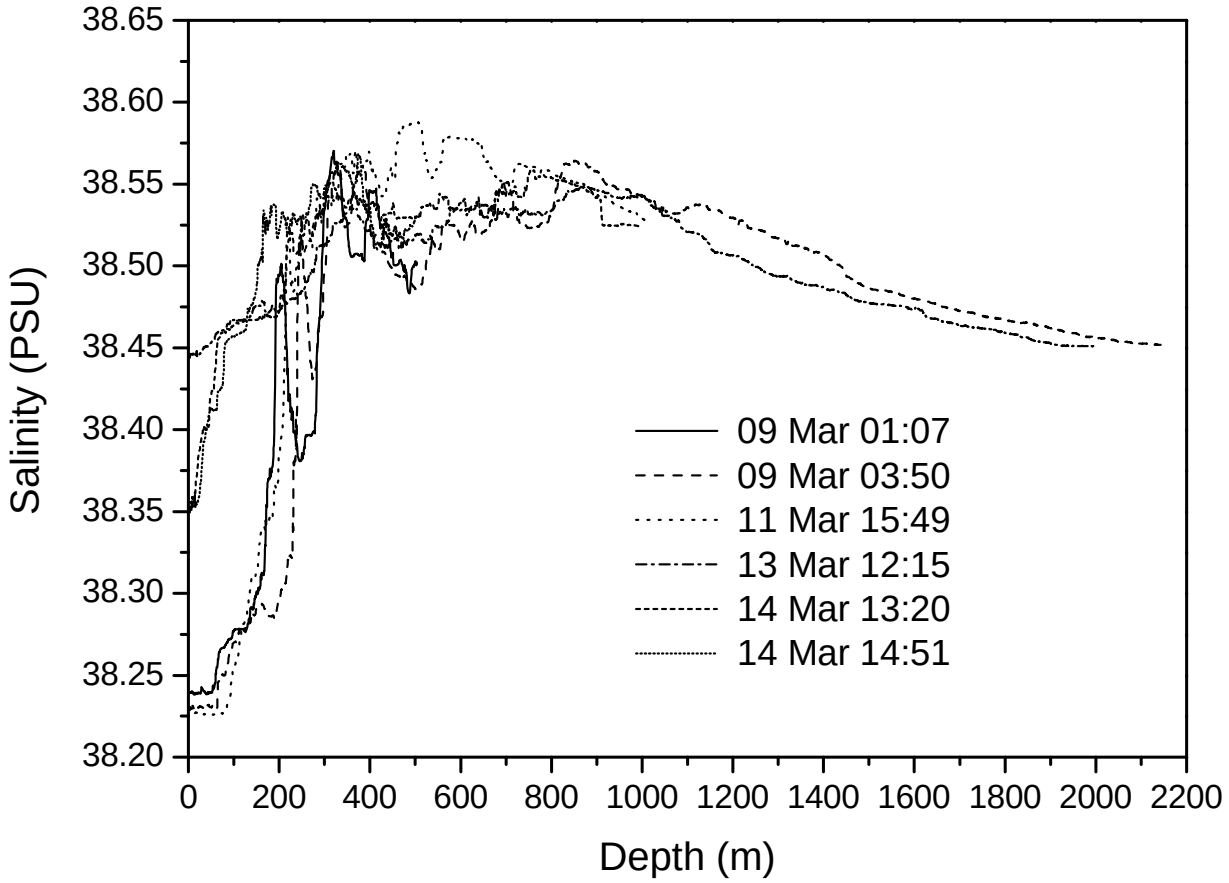
Salinity (PSU)
38.65
38.60
38.55
38.50
38.45
38.40
38.35
38.30
38.25
38.20
0
200
400
600
800
1000
1200
1400
1600
1800
2000
2200
Depth (m)
09 Mar 01:07
09 Mar 03:50
11 Mar 15:49
13 Mar 12:15
14 Mar 13:20
14 Mar 14:51

Figure 4a

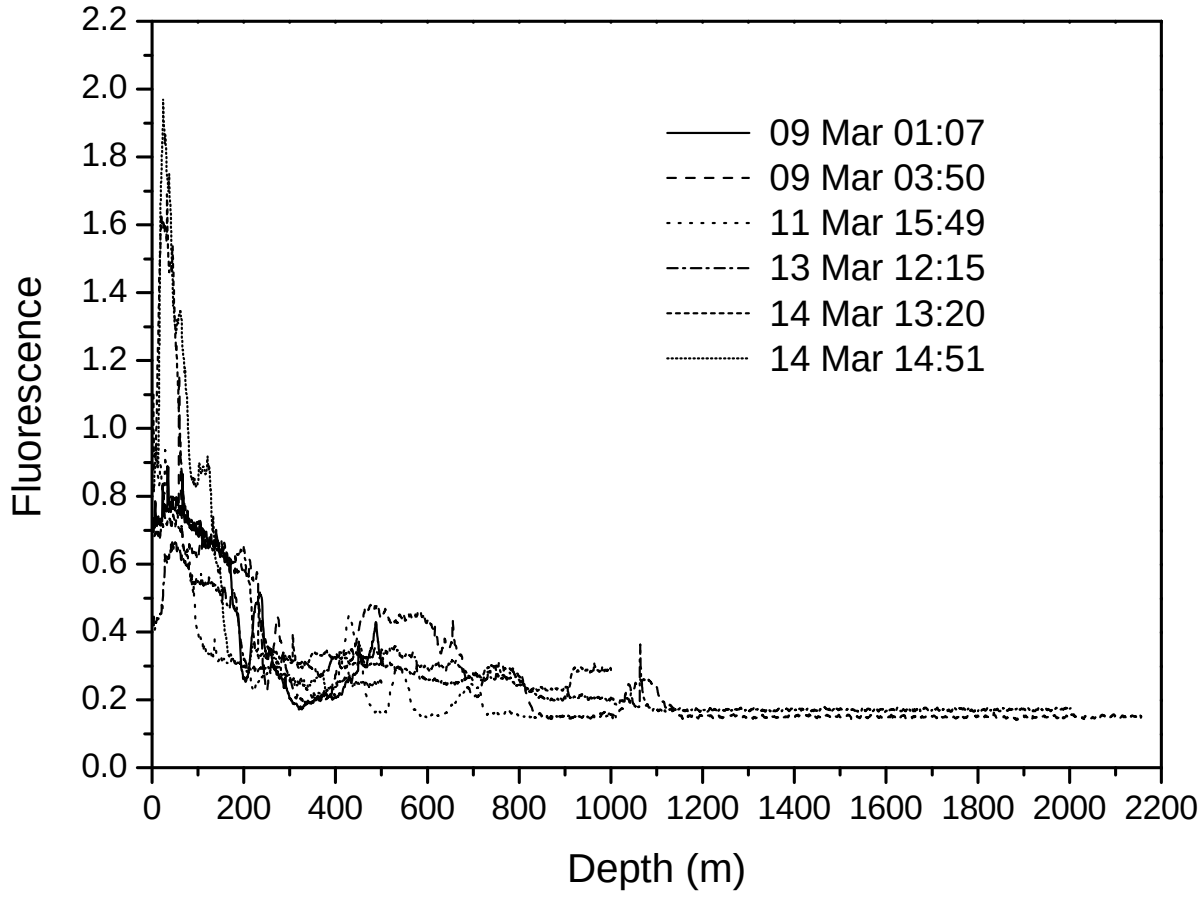
Fluorescence
Depth (m)
09 Mar 01:07
09 Mar 03:50
11 Mar 15:49
13 Mar 12:15
14 Mar 13:20
14 Mar 14:51
0.0
0.2
0.4
0.6
0.8
1.0
1.2
1.4
1.6
1.8
2.0
2.2
0
200
400
600
800
1000
1200
1400
1600
1800
2000
2200

Figure 4b

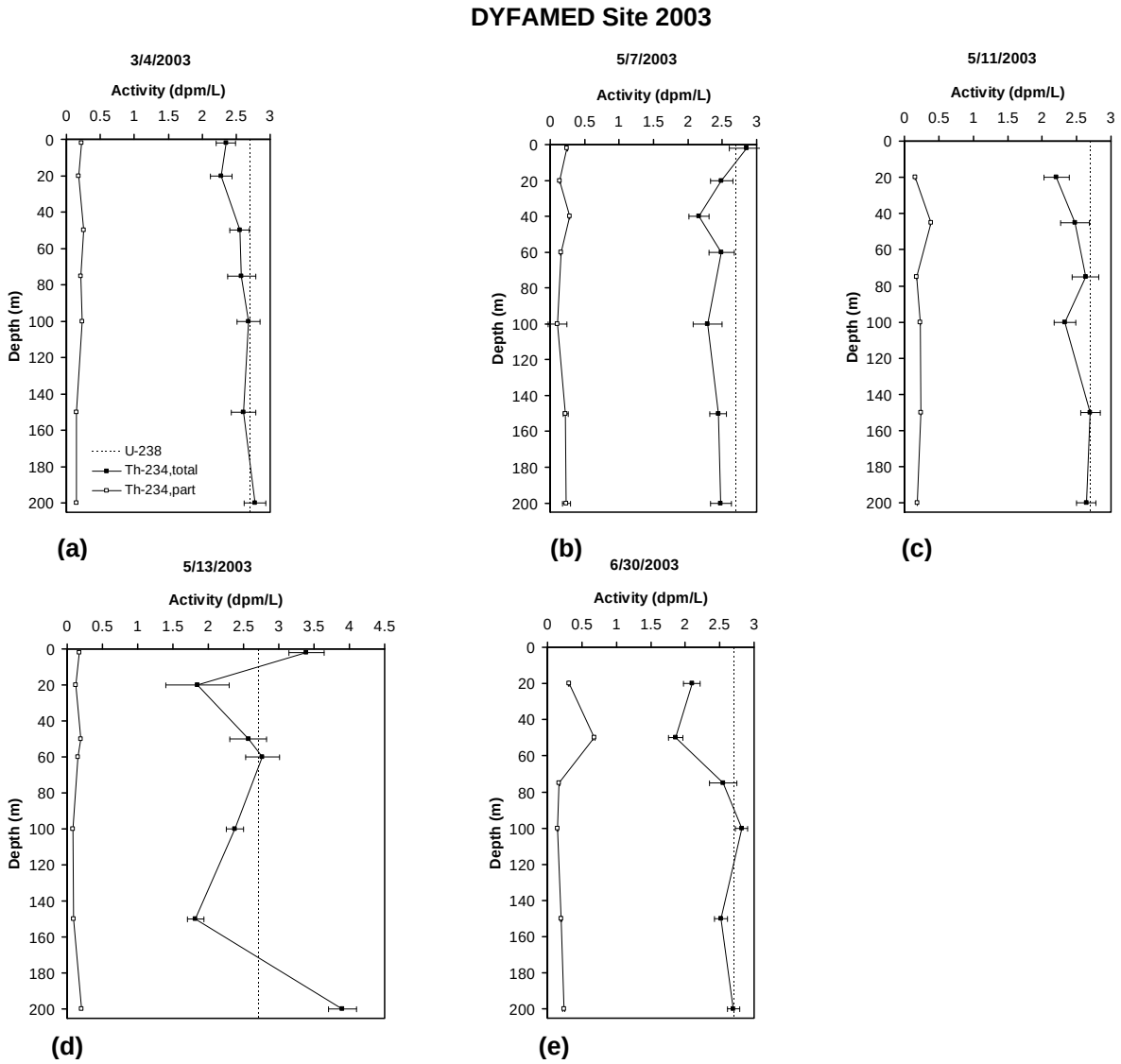
DYFAMED Site 2003
3/4/2003
5/7/2003
5/11/2003
5/13/2003
6/30/2003
Activity (dpm/L)
Depth (m)
U-238
Th-234,total
Th-234,part
(a)
(b)
(c)
(d)
(e)

Figure 5

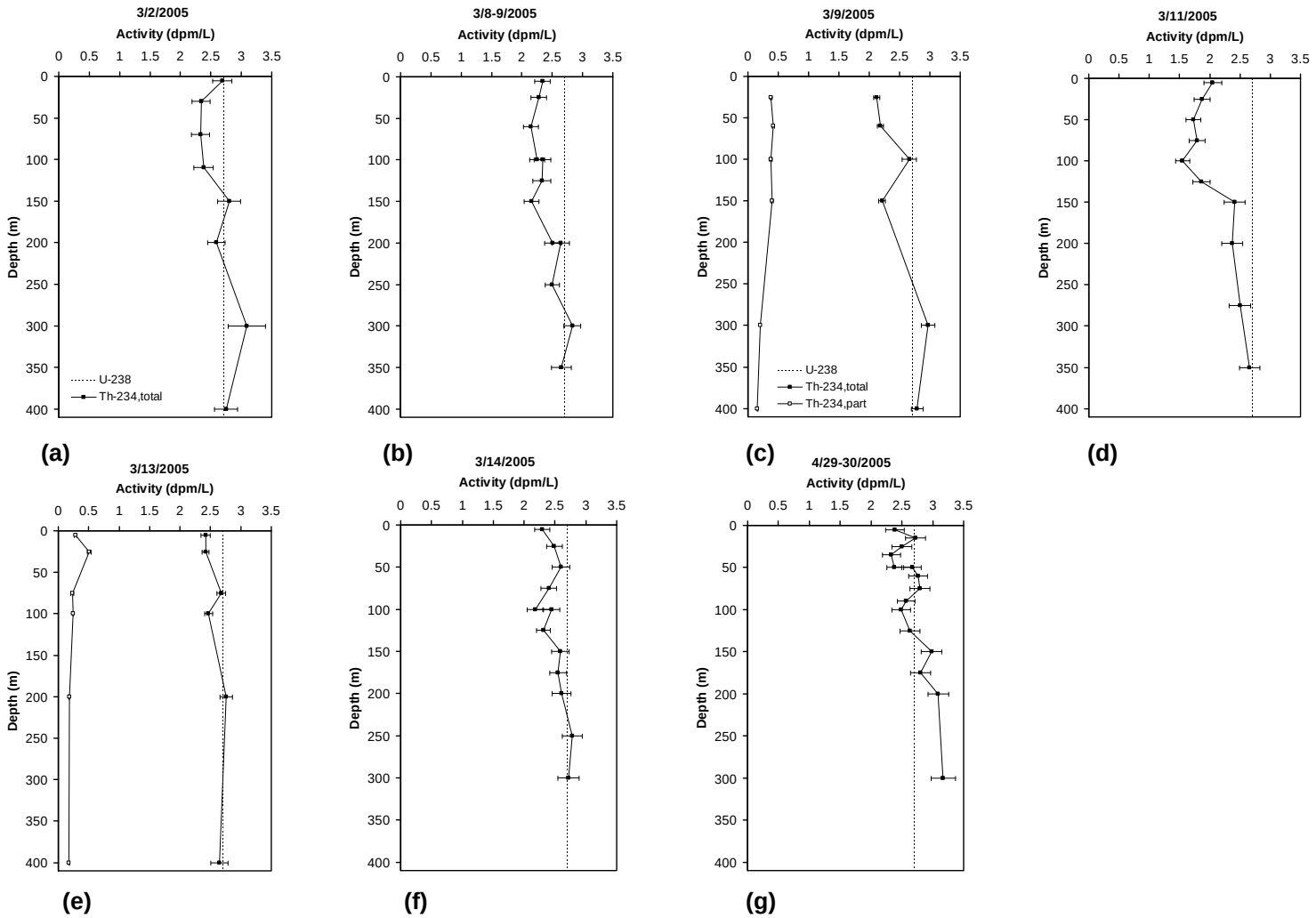
DYFAMED Site 2005
3/2/2005
3/8-9/2005
3/9/2005
3/11/2005
3/13/2005
3/14/2005
4/29-30/2005
Activity (dpm/L)
Depth (m)
U-238
Th-234,total
Th-234,part
(a)
(b)
(c)
(d)
(e)
(f)
(g)

Figure 6

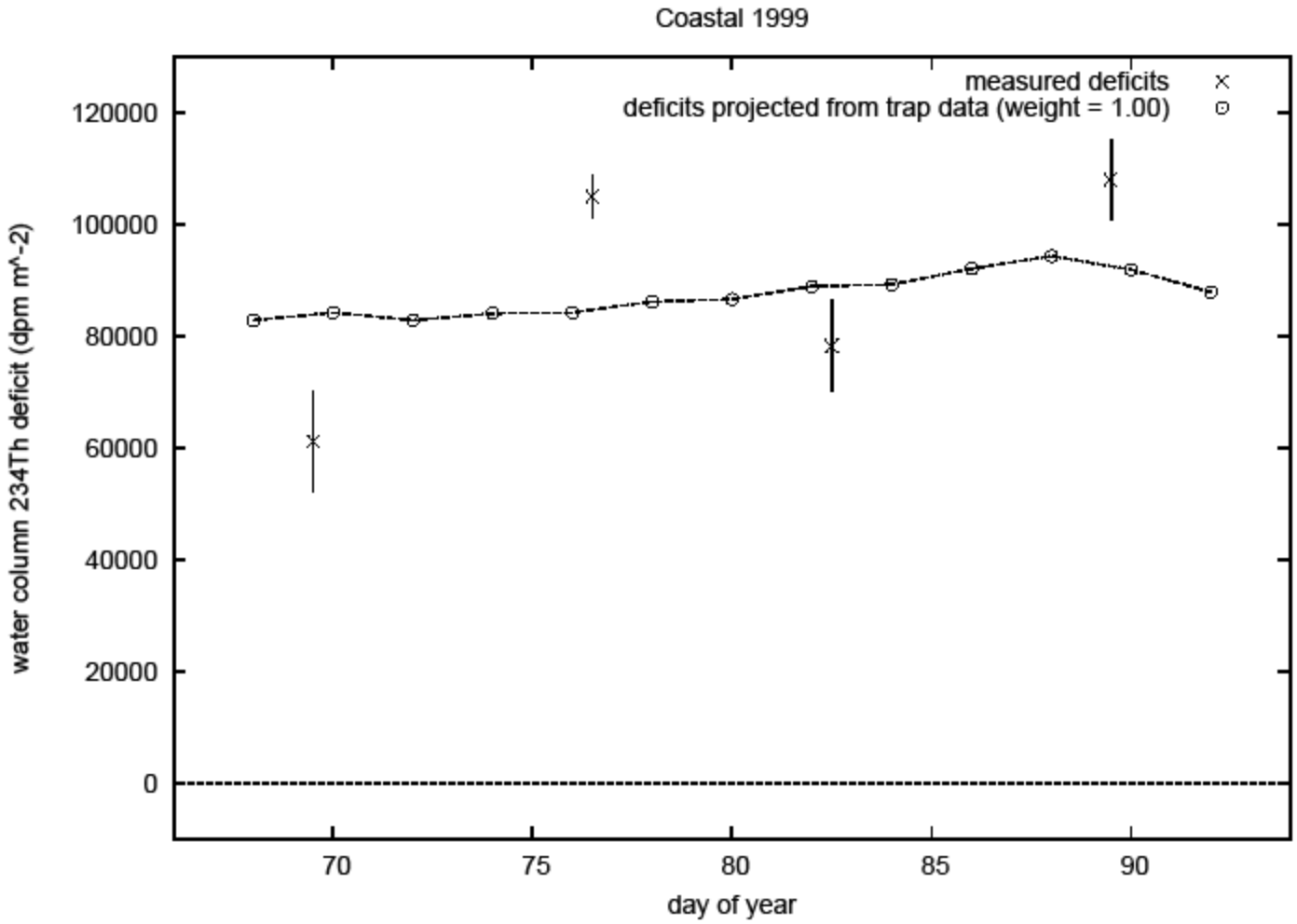
Coastal 1999
measured deficits
deficits projected from trap data (weight = 1.00)
water column 234Th deficit (dpm m^-2)
120000
100000
80000
60000
40000
20000
0
70
75
80
85
90
day of year

Figure 7

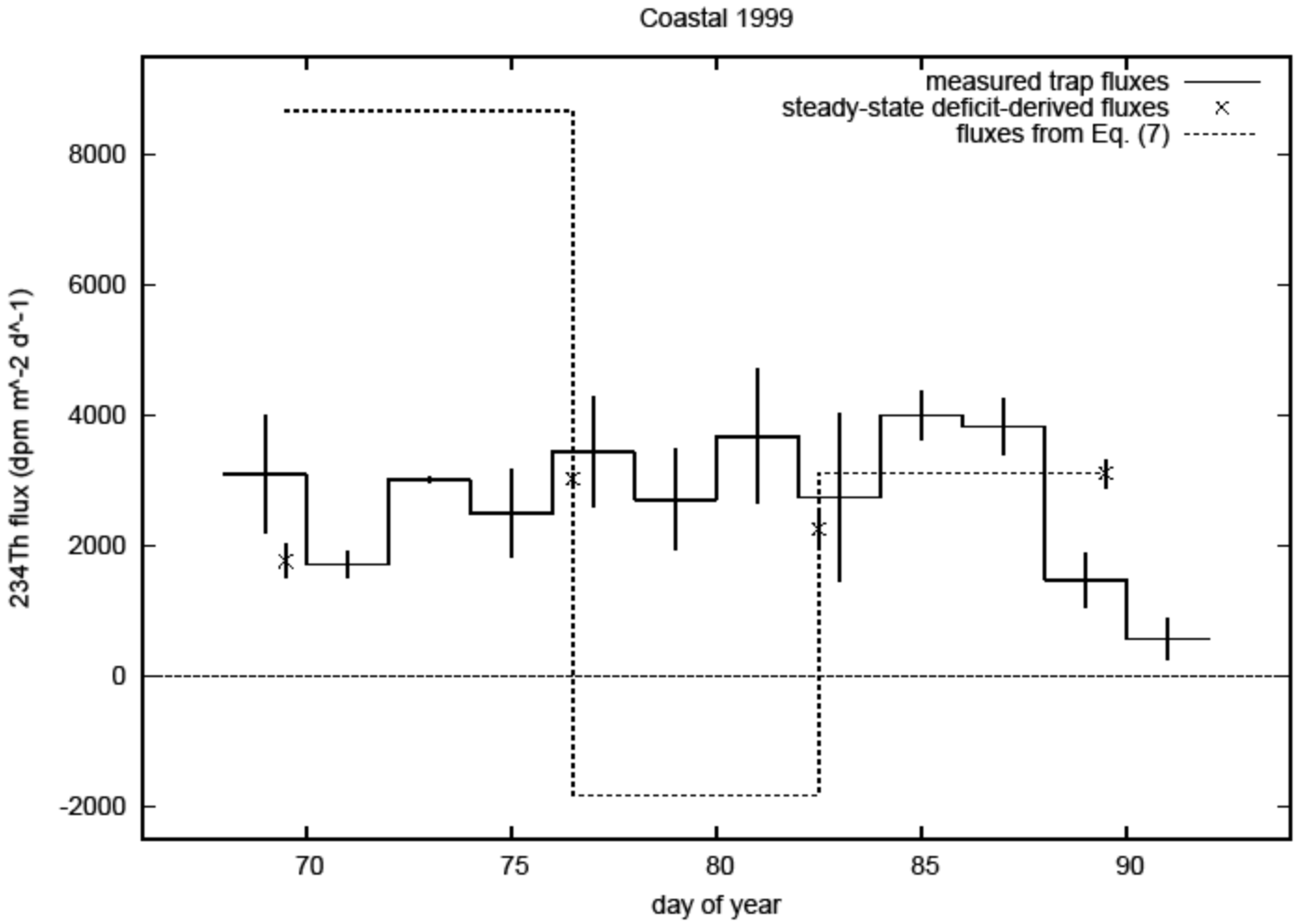
Coastal 1999
measured trap fluxes
steady-state deficit-derived fluxes
fluxes from Eq. (7)
234Th flux (dpm m^-2 d^-1)
8000
6000
4000
2000
0
-2000
70
75
80
85
90
day of year

Figure 8

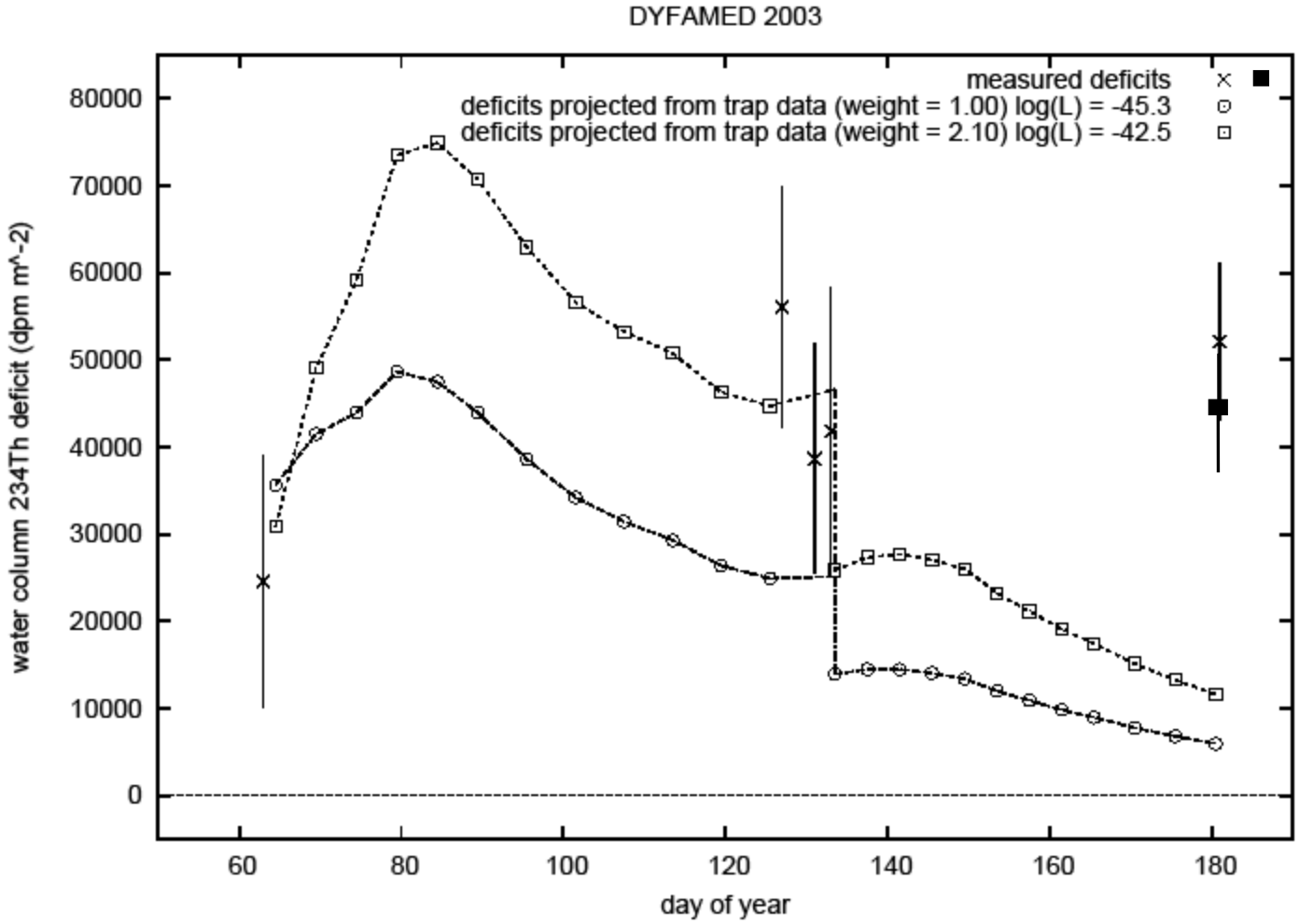
DYFAMED 2003
measured deficits
deficits projected from trap data (weight = 1.00) log(L) = -45.3
deficits projected from trap data (weight = 2.10) log(L) = -42.5
water column 234Th deficit (dpm m^-2)
80000
70000
60000
50000
40000
30000
20000
10000
0
60
80
100
120
140
160
180
day of year

Figure 9

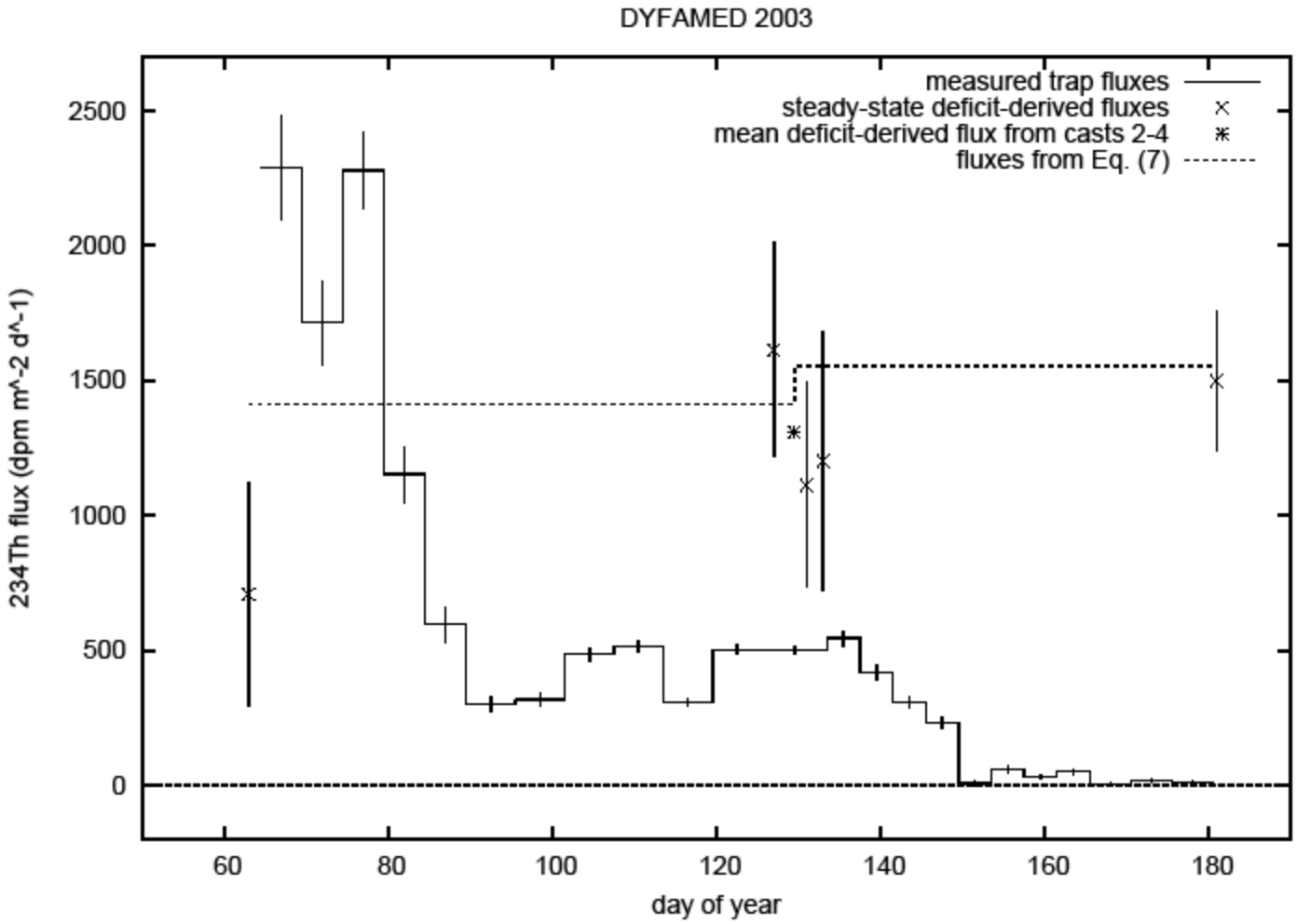
DYFAMED 2003
measured trap fluxes
steady-state deficit-derived fluxes
mean deficit-derived flux from casts 2-4
fluxes from Eq. (7)
234Th flux (dpm m^-2 d^-1)
2500
2000
1500
1000
500
0
60
80
100
120
140
160
180
day of year

Figure 10

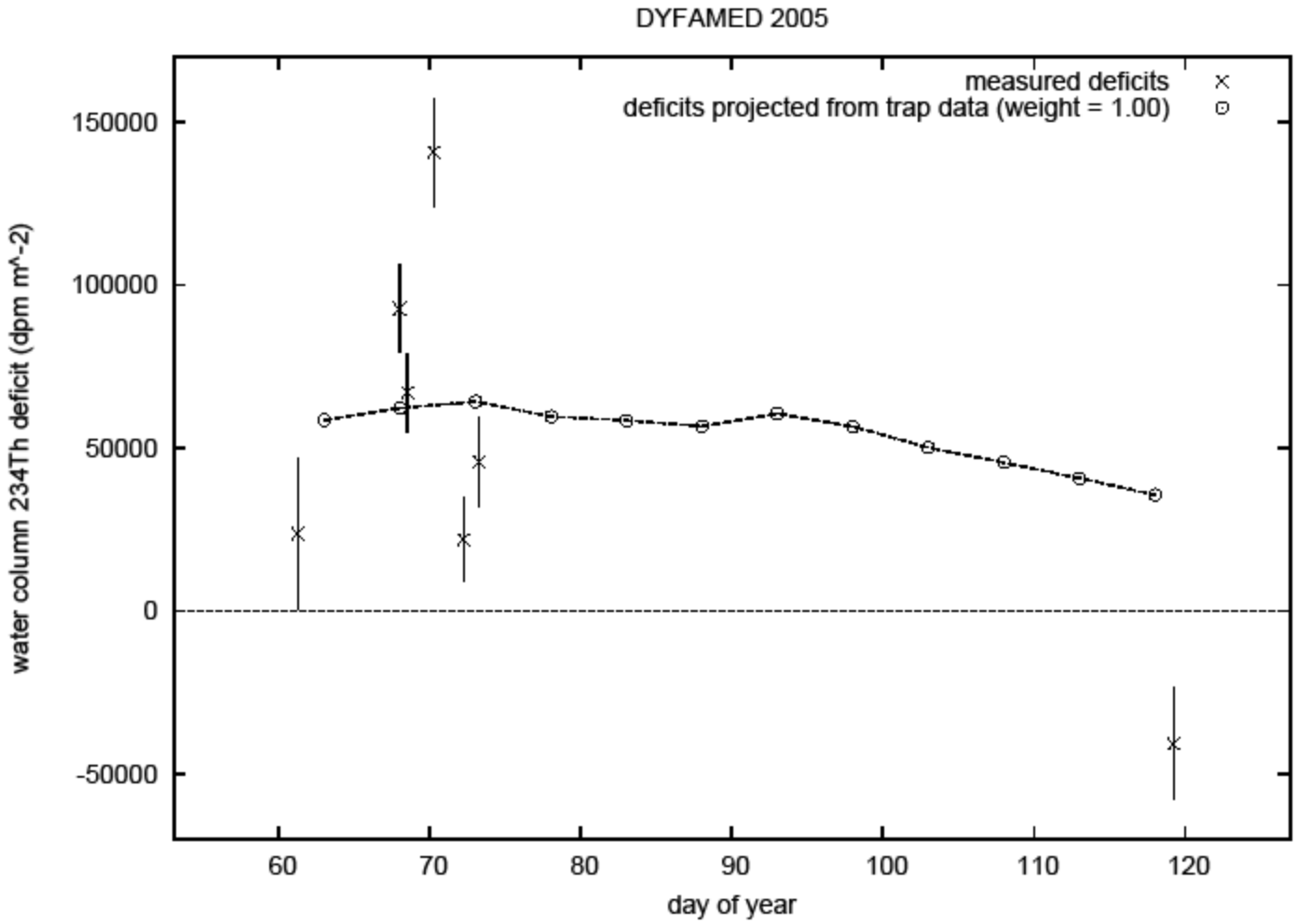
DYFAMED 2005
measured deficits
deficits projected from trap data (weight = 1.00)
water column 234Th deficit (dpm m^-2)
150000
100000
50000
0
-50000
60
70
80
90
100
110
120
day of year

Figure 11

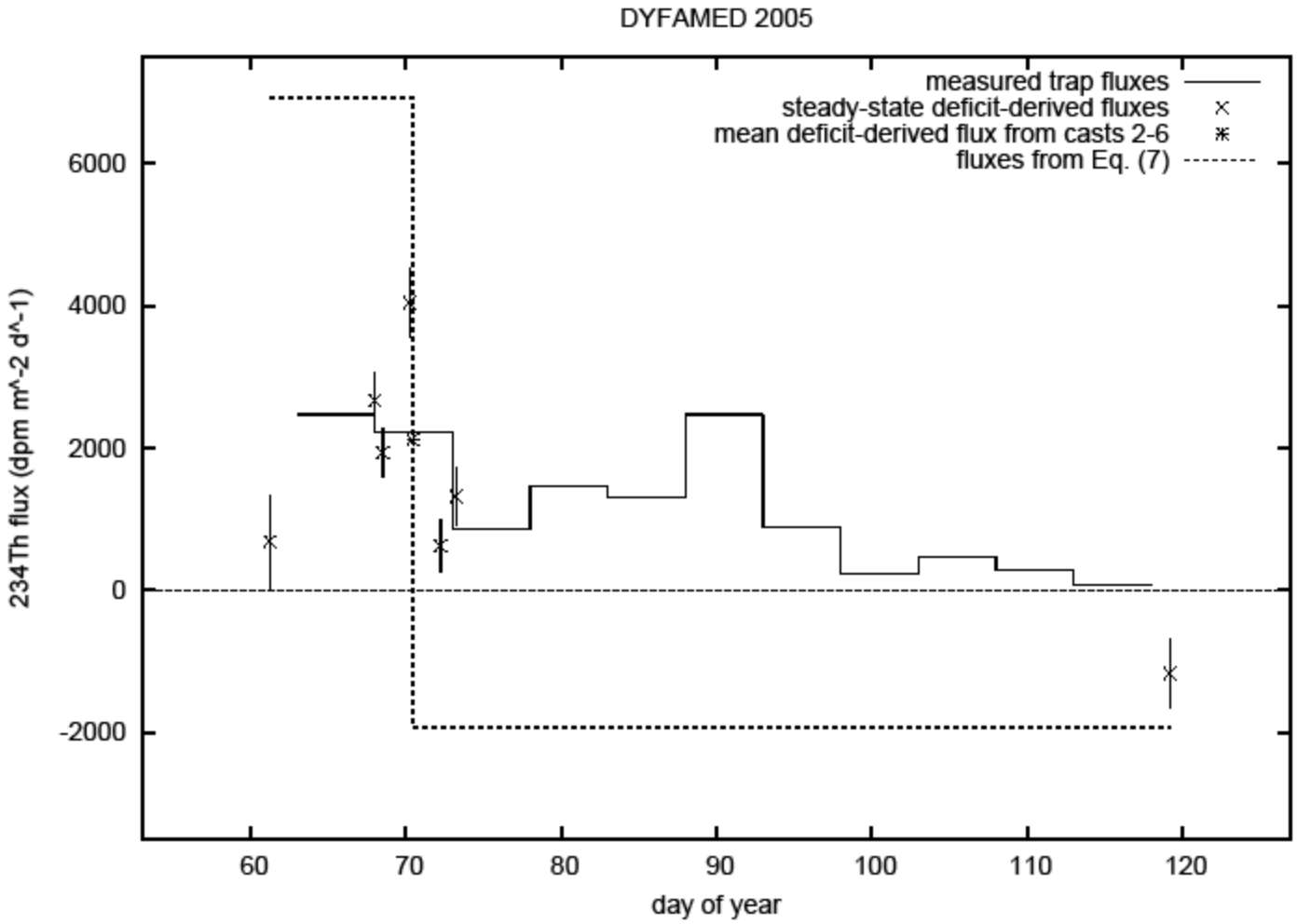
DYFAMED 2005
measured trap fluxes
steady-state deficit-derived fluxes
mean deficit-derived flux from casts 2-6
fluxes from Eq. (7)
234Th flux (dpm m^-2 d^-1)
6000
4000
2000
0
-2000
60
70
80
90
100
110
120
day of year

Figure 12